(O'Callaghan *et al.*, 1999; Sieira *et al.*, 2000). This operon is composed of 13 open reading frames (ORFs) that share homology with other bacterial type IV secretion systems known to be involved in the intracellular trafficking of pathogens, for example the *dot/icm* genes of *L. pneumophila*. An in-frame, deletion mutation introduced in the fourth gene of the operon, *virB4*, abolished the ability of *Brucella* to target properly and replicate intracellularly, indicating that this system is essential for the intracellular lifestyle of this pathogen (Watarai *et al.*, 2002). Mice infected with polar and non-polar mutations in *virB10* and an in-frame deletion mutation in *virB4* demonstrated that the *virB* operon is a major determinant of *Brucella* virulence (Sieira *et al.*, 2000; Watarai *et al.*, 2002). Thus, the VirB proteins of *Brucella abortus* are thought to be constituent elements of the secretion apparatus, but the molecular basis of these mechanisms is unknown.

Among the events influencing the fate of phagosomes, the type of infected cell and the uptake route are clearly of importance (Sinai and Joiner, 1997). Several processes have been described for the internalization of intracellular pathogens. *Legionella pneumophila* enters cells by coiling phagocytosis, a phenomenon characterized by the formation of pseudopods that coil around the bacterium (Horwitz, 1984). Recently, it has been reported that *L. pneumophilla* was internalized by a macropinocytotic uptake pathway and that the macropinosomes containing *L. pneumophila* were rich in GM1 gangliosides and GPI-anchored proteins. The uptake pathway is controlled by the Dot/Icm system and the mouse *Lgn1* locus (Watarai *et al.*, 2001a). *Listeria* or *Yersinia* internalization occurs by zipper-like phagocytosis in which bacterial surface proteins bind to host cell surface receptors (Isberg, 1996; Lecuit *et al.*, 1999). Other bacteria, such as *Salmonella* and *Shigella*, invade by a trigger mechanism into professional and non-professional phagocytes (Bourdet-Sicard *et al.*, 2000). These pathogens deliver virulence factors directly into the target host cell cytosol, triggering host cell signalling pathways that lead to localized plasma membrane ruffling, macropinocytosis and bacterial uptake (Galan, 2000). On the other hand, the uptake route of *B. abortus* remains unknown.

In this report, we describe a similar phagocytic pathway to *L. pneumophilla* promoted by the VirB system of *B. abortus*. The pathway appears similar to macropinocytosis associated with recruitment of lipid rafts. By incorporation of the lipid raft-associated components into macropinosomes containing *B. abortus*, a replicative phagosome is established. This indicates that the internalization strategy of *B. abortus* into macrophage is involved in controlling correct targeting and intracellular growth.

Results

Bacterial swimming after contact of macrophages with B. abortus *is dependent on the* virB *genes*

Time-lapse videomicroscopy was used to follow the internalization of GFP-expressing *B. abortus* strains by mouse bone marrow-derived macrophages. After contact of macrophages with the strain harbouring an intact VirB system (Ba600), bacteria moving round from the site of initial bacterial contact with the macrophage were observed (Fig. 1A). The swimming of the bacteria on the macrophage surface often lasted for up to 8 min with generalized plasma membrane ruffling before eventual enclosure in large vacuoles (Fig. 1A). Contact of Ba604 (Δ*virB4*) with the target macrophage, in contrast, resulted in much smaller ruffling that was restricted to the area near the bacteria. The ruffles associated with internalization of Ba604 (Δ*virB4*) resulted in a more rapid uptake than observed for Ba600 (wild type), with the bacteria moving out of the focal plane of the site of bacterial binding, apparently signifying internalization underneath a phase opaque structure (Fig. 1B).

To obtain further comparisons between wild-type and mutant strains, an alternative procedure was used to determine morphological changes induced in the macrophage after contact with *B. abortus*. To this end, bacteria were deposited onto macrophages by centrifugation, and stained with phalloidin to detect actin filament formation using fluorescence microscopy. Five minutes after deposition on the macrophages, Ba600 (wild type) showed generalized actin polymerization around the site of bacterial binding, which could be observed by either phalloidin staining or phase-contrast microscopy (Fig. 1C). Ba604 (Δ*virB4*) showed primarily small regions of phalloidin staining at sites of binding (Fig. 1C). Therefore, *B. abortus* appears to promote events on the macrophage cell surface that are dependent on the presence of the VirB system.

Macropinocytosis induced by B. abortus *is dependent on the* virB *genes*

Based on analysis of time-lapse videomicroscopy, it also appeared that after induction of generalized membrane ruffling, the bacteria were internalized into large vacuoles. To analyse this further, samples were fixed after brief incubation of mouse bone marrow-derived macrophages with *B. abortus*. For Ba600 (wild type), the bacteria were found in large concentric vacuoles that were similar in morphology to fluid-filled macropinosomes (Swanson, 1989). Macrophages incubated simultaneously with *B. abortus* and the fluid phase marker (tetramethyl rhodamine isothiocyanate) TRITC-Dextran (TRDx) accumulated the marker

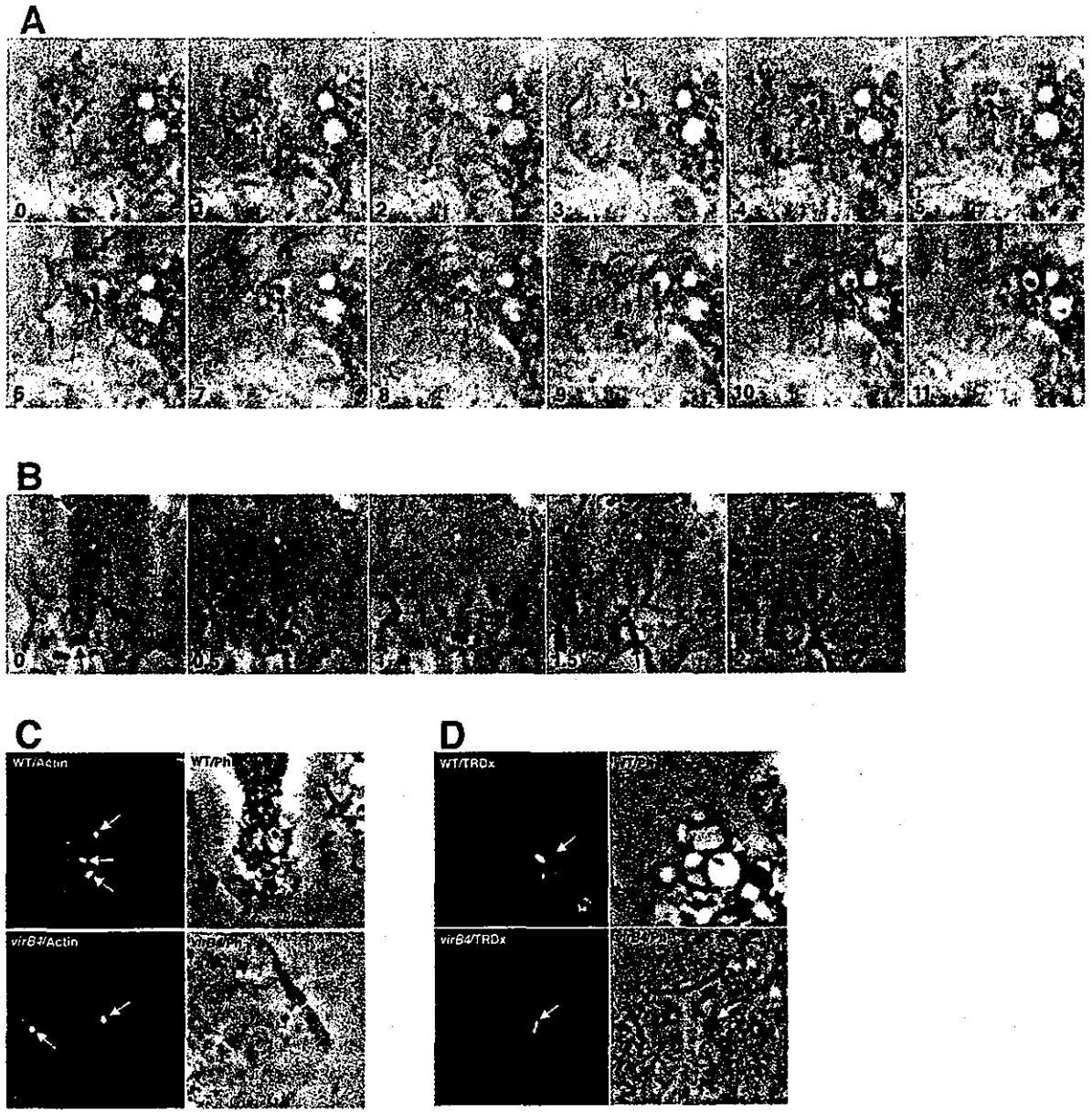

Fig. 1. Uptake process of *B. abortus* by mouse bone marrow-derived macrophages. Selected time-lapse videomicroscopic images of *B. abortus* entry into the macrophage. Elapsed time in minutes is indicated at the bottom of each frame. Arrows point to bacteria.
A. Ba600 (wild type) observed after contact with macrophage. Note bacterial swimming with generalized membrane ruffling from 0 to 8 min, and the bacterium inside macropinosme at 10–11 min.
B. Ba604 (Δ*virB4*) observed after contact with macrophage. Note phase opaque ruffle associated with bacterial contact.
C. Generalized actin polymerization after contact of macrophages with *B. abortus*. Bacteria were deposited onto macrophages and then incubated for 5 min, fixed and stained for actin filaments with Alexa Fluor 594-phalloidin. Incubations with Ba600 (wild type) (upper panels) and Ba604 (Δ*virB4*) (lower panels) stained by phalloidin are displayed. Shown are GFP and Alexa Flour 594 channels merged or phase-contrast images.
D. Macropinosome formation by *B. abortus*. Macrophages were incubated for 15 min at 37°C in the presence of Ba600 (wild type) (upper panels) or Ba604 (Δ*virB4*) (lower panels) and TRDx, fixed and processed for phase and immunofluorescence microscopy. Shown are GFP and rhodamine channels merged or phase images.

in large vacuoles containing Ba600 (wild type) whereas little or no marker accumulated in phagosomes harbouring Ba604 (Δ*virB4*) (Fig. 1D). Similarly, phase-contrast micrographs showed Ba600 (wild type) in large phase-transparent compartments, whereas Ba604 (Δ*virB4*) was found in considerably smaller compartments (Fig. 1D).

The differences in rate of phagocytosis and the formation of macropinosomes for wild-type and mutant strain

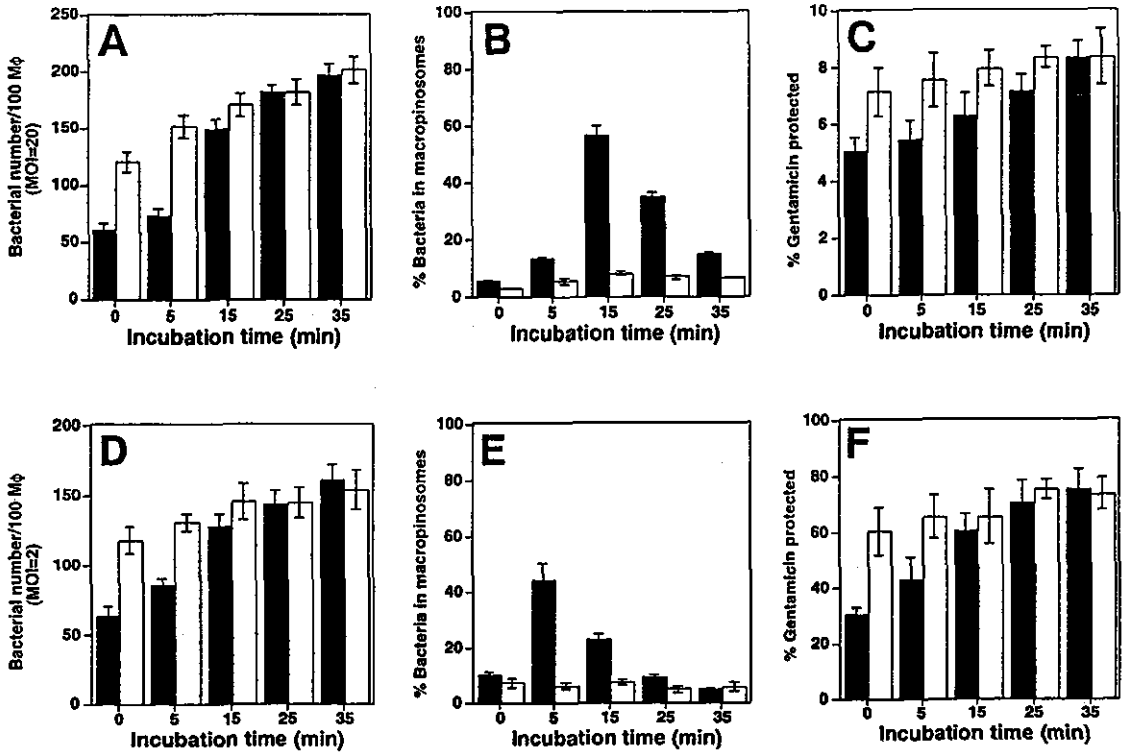

Fig. 2. Delayed phagocytosis and macropinosome formation promoted by the *B. abortus* VirB system. Bacteria were deposited onto bone marrow-derived macrophages and incubated at 37°C for the periods of time indicated. Uptake (A, C, D and F) or macropinosome formation (B and E) were quantitated as described (see *Experimental procedures*). A–C, no opsonization; D–F, opsonization with anti-*B. abortus* serum (see *Experimental procedures*); A, B, D and E, 100 macrophages were examined per coverslip; C and F, uptake efficiency by macrophages was determined by protection of internalized bacteria from gentamicin killing. Black bars, Ba600 (wild type); open bars, Ba604 (Δ*virB4*). Data are the average of triplicate samples from three identical experiments, and the error bars represent the standard deviation.

were quantitated microscopically at various times of incubation, using strategies that allowed as synchronous an infection as possible (see *Experimental procedures*). If the bacteria were deposited onto macrophages by centrifugation, Ba604 (Δ*virB4*) was rapidly internalized, with most of the associated bacteria internalized before further incubation at 37°C. In contrast, internalization of Ba600 (wild type) was delayed and attained the same levels of internalization as Ba604 (Δ*virB4*) only after 25 min incubation (Fig. 2A). In regards to macropinosome formation, by 15 min after deposition of Ba600 (wild type), 56% of the bacteria were found in large compartments containing TRDx that could be detected by phase-contrast microscopy. The ability to observe macropinosomes decayed after this time point, with few bacteria costaining with TRDx at 35 min post infection. Phagosomes harbouring Ba604 (Δ*virB4*), on the other hand, were relatively devoid of the fluid phase marker (Fig. 2B).

Delayed phagocytosis rate and transient macropinosome formation did not require a particular strategy of bacterial contact with the macrophage. Opsonization increased both the rate and total amount of uptake for each strain, but the total amount of internalized Ba600 (wild type) was still less than that observed for Ba604 (Δ*virB4*) until 15 min incubation (Fig. 2D). In addition, the rate of appearance of VirB-dependent macropinosomes was enhanced by opsonization, with macropinosomes surrounding approximately 44% of those analysed at the earlier time point. As had been observed with unopsonized bacteria, the morphology of the macropinosomes changed rapidly, since almost no macropinosomes were observed after 35 min of incubation (Fig. 2E).

The above observations were confirmed by assaying for viable bacteria, protected from gentamicin killing, within macrophages. Delayed uptake rate was observed for Ba600 (wild type) relative to Ba604 (Δ*virB4*) (Figs 2C–F).

In addition to the in-frame deletion mutation in *virB4*, mutant *virB4* altered in the NTP-binding region by site-directed mutagenesis (Watarai *et al.*, 2002), and a strain harbouring an in-frame deletion in *virB2* failed to form macropinosomes and had higher uptake efficiencies than the wild-type strain (data not shown). This observation is consistent with some aspect of the VirB machinery functioning to promote formation of a specialized uptake pathway.

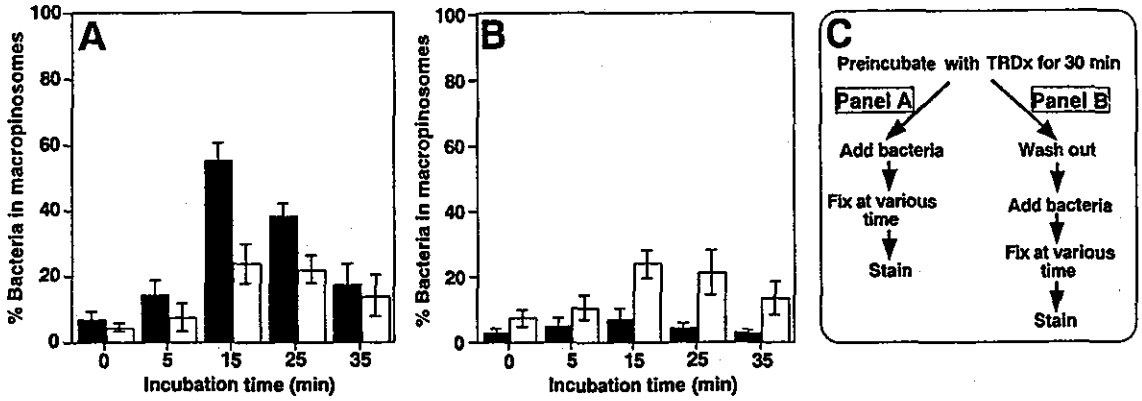

Fig. 3. Compartments preloaded with a fluid phase marker do not fuse with macropinosomes containing *B. abortus* with intact VirB system. Bone marrow-derived macrophages were incubated with 1 mg ml^{-1} TRDx for 30 min at 37°C and then incubated with bacteria either in the continued presence (A) or absence (B) of the fluid phase marker (see panel C). Number of bacteria in compartments staining with TRITC was determined as described (see *Experimental procedures*). Black bars, Ba600 (wild type); open bars, Ba604 (Δ*virB4*). Data are the average of triplicate samples from three identical experiments, and the error bars represent the standard deviation.

Macropinosomes containing B. abortus *avoid fusion with another macropinosomes*

To examine the intracellular trafficking of macropinosomes containing *B. abortus*, macrophages were preloaded for 30 min with TRDx before addition of *B. abortus*, and infection allowed to proceed either in the presence or absence of the marker (Fig. 3C). As expected, if the bacteria were added in the continued presence of the marker, colocalization of TRDx with Ba600 (wild type) was similar to that observed when there was no preincubation of TRDx before infection. The behaviour of Ba604 (Δ*virB4*), however, was different than in the previous protocol. At 15 min post infection, there was transient colocalization of TRDx with Ba604 (Δ*virB4*), implying that the marker accumulated in an intracellular compartment that could fuse with Ba604 (Δ*virB4*) but not with Ba600 (wild type) (Fig. 3A). To confirm this, TRDx was washed out of the medium before the addition of bacteria. Colocalization of the marker with Ba600 (wild type) was almost completely lost. In contrast, removing the fluid phase marker before the addition of Ba604 (Δ*virB4*) gave results that were similar to those observed with continued incubation of TRDx during the infection, with transient colocalization of TRDx (Fig. 3B). These results are consistent with Ba600 (wild type) being simultaneously ingested with TRDx into a fluid-filled phagosome that resists fusion with marker-filled compartments. In contrast, phagosomes harbouring Ba604 (Δ*virB4*) formed without simultaneous ingestion of TRDx, but were able to fuse with marker-filled compartments after internalization.

Incorporation of lipid raft-associated components into macropinosomes containing B. abortus

Previous studies have demonstrated that *B. abortus* may alter the maturation of its phagosome before fusion with late endosomes, thus preventing the acquisition of late endosomal and lysosomal markers LAMP-1 and cathepsin D (Pizarro-Cerda *et al.*, 1998a, b; Watarai *et al.*, 2002). To this end, bacterial phagosomes were scored for acquisition of LAMP-1. As reported previously (Watarai *et al.*, 2002), more than 80% of the phagosomes and 90% of the macropinosomes containing Ba600 (wild type) failed to colocalize with LAMP-1 in bone marrow-derived macrophages after 15–35 min incubation, whereas Ba604 (Δ*virB4*) was found predominantly colocalized with LAMP-1 (Figs 4A and F; Figs 6A and G). Therefore, macropinocytotic uptake of *B. abortus* is correlated with an ability of the phagosome to avoid interaction with the endocytic pathway..

In addition, aerolysin from *Aeromonas hydrophila*, which binds to GPI-anchored proteins on the cell surface (Abrami *et al.*, 1998; Wang *et al.*, 1999), affected the replicative phagosomes harbouring *B. abortus* (Pizarro-Cerda *et al.*, 1998a). To determine if GPI-anchored proteins were incorporated into macropinosomes containing *B. abortus*, the macropinosomes were probed with aerolysin. The kinetics and degree of association of aerolysin-labelled GPI-anchored proteins with internalized Ba600 (wild type) showed maximal association after 15 min incubation at 37°C (Figs 5A, B and 6B). Moreover, the association of aerolysin-labelled GPI-anchored proteins with internalized Ba600 (wild type) showed remarkably high efficiency in macropinosomes (77%, Fig. 6G). In contrast, colocalization of aerolysin-labelled GPI-anchored proteins with Ba604 (Δ*virB4*) was much less pronounced (Fig. 6B). Consistent with these results, GPI-anchored protein CD48 was incorporated into macropinosomes containing Ba600 (wild type) (Figs 4C, H and Fig 6G), and similar kinetics results were obtained for the aerolysin-labelled GPI-anchored proteins from both strains (Fig. 6D). On the other hand, transmembrane

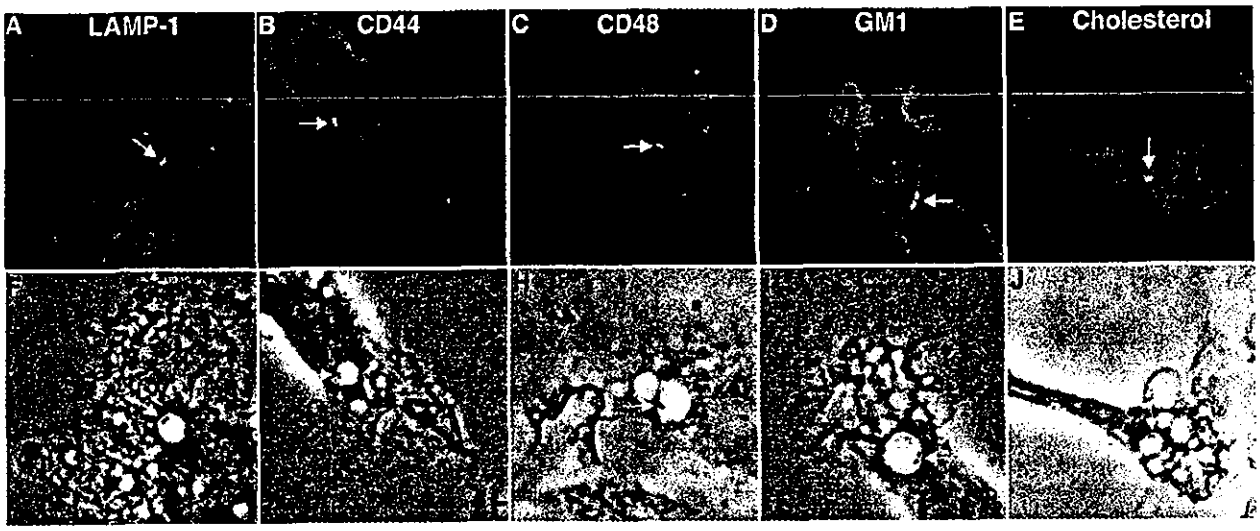

Fig. 4. Association of membrane-localized markers with *B. abortus* macropinosomes. Bone marrow-derived macrophages were incubated with *B. abortus*, and membrane-associated markers were localized by immunofluorescence, as described (see *Experimental procedures*). Shown are merged images of the GFP and TRITC (A–D) or UV (F) channels up-and-down with phase-contrast images of the identical cells (F–J). Cells were probed with anti-LAMP-1 (A and F), anti-CD44 (B and G), anti-CD48 (C and H), CTB for GM1 gangliosides (D and I) or filipin for cholesterol (E and J). Arrows point to bacteria.

protein CD44 was found associated with ruffles in the plasma membrane above the vacuole, but was excluded from macropinosomes containing Ba600 (wild type) (Figs 4B, G and 6C). These results suggested that sphingolipid-cholesterol-rich microdomains, lipid rafts, might be incorporated into the macropinosome containing *B. abortus*.

To investigate this possibility, the macropinosomes were probed with other components known to be associated with lipid rafts, such as GM1 gangliosides and cholesterol. To this end, *B. abortus* and biotin-labelled cholera toxin B subunit (CTB), which binds GM1-gangliosides, were incubated simultaneously with macrophages. CTB

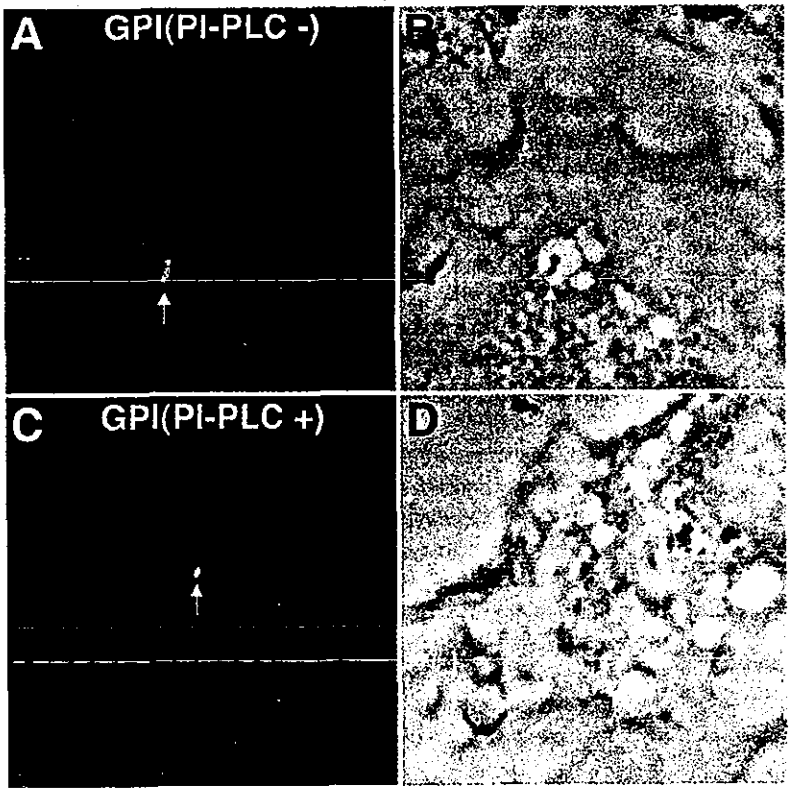

Fig. 5. Association of GPI-anchored proteins with *B. abortus* macropinosomes. Bone marrow-derived macrophages were incubated with *B. abortus*, and aerolysin-labelled GPI-anchored proteins were localized in the presence (C and D) or absence (A and B) of PI-PLC by immunofluorescence, as described (see *Experimental procedures*). Shown are merged images of the GFP and TRITC (A and C) channels side-by-side with phase-contrast images of the identical cells (B and D). Arrows point to bacteria.

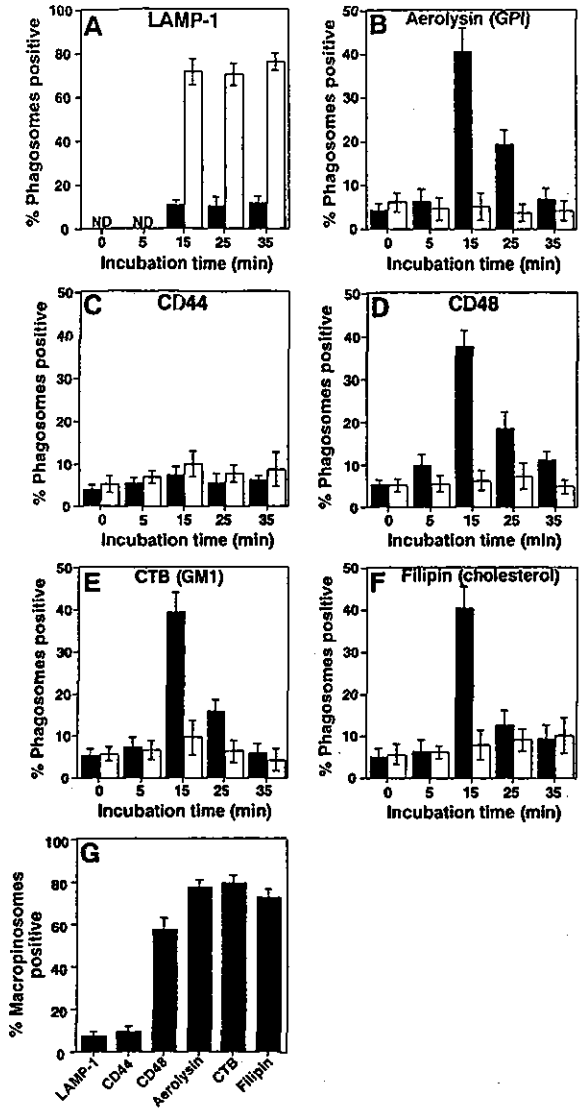

Fig. 6. Kinetics of colocalization of membrane-associated markers with phagosomes containing *B. abortus*. (A-F): Ba600 (wild type) (black bars) or Ba604 (Δ*virB4*) (open bars) were deposited onto macrophages, then incubated for the periods of time indicated at 37°C before fixation and probing with indicated reagents (see *Experimental procedures*). '%Phagosomes positive' refers to percentage of internalized bacteria that showed co-staining with the noted markers, based on observation of 100 bacteria per coverslip. A, anti-LAMP-1; B, aerolysin for GPI-anchored proteins; C, anti-CD44; D, anti-CD48; E, CTB for GM1 gangliosides; F, filipin for cholesterol. Data are the average of triplicate samples from three identical experiments, and the error bars represent the standard deviation. ND, not detectable. G. Macrophages incubated with Ba600 (wild type) for 15 min at 37°C were probed for noted markers, and macropinosomes harbouring Ba600 (wild type) were identified by fluorescence and phase microscopy. The macropinosomes were then observed for the presence of the noted markers, as in A–F. '% Macropinosomes positive' refers *only* to those phagosomes with a macropinocytotic morphology, and represents the percentage of macropinosomes that show costaining with the noted markers. Data for macropinosomes are from triplicate coverslips representing 50 macropinosomes per coverslip, and the error bars represent the standard deviation.

was found to localize around the internalized Ba600 (wild type) with kinetics of association similar to those observed for aerolysin-labelled GPI-anchored proteins. In contrast, colocalization of CTB with Ba604 (Δ*virB4*) was much less pronounced (Fig. 6E). As was true for aerolysin-labelled GPI-anchored proteins, if only the subset of bacteria found in macropinosomes were analysed, 79% of the macropinosomes were found to have co-internalized CTB and Ba600 (wild type) (Figs 4D, I and 6G). To probe for cholesterol known to be raft-associated, macrophages infected with *B. abortus* were fixed and probed with the fluorescent cholesterol-binding drug filipin (Mukherjee *et al.*, 1998). The kinetics of association of cholesterol, based on this assay, were almost identical to those observed for CTB-labelled GM1-gangliosides colocalization (Fig. 6F), with the staining of the vacuoles being remarkably intense (Figs 4E and 4J). As was true for aerolysin and CTB, if only Ba600 (wild-type)-bearing macropinosomes were analysed, colocalization was abundant, with close to 72% of the vacuoles staining with filipin (Fig. 6G). These results indicated that formation of the VirB-dependent macropinosome involved a sorting process that allowed the transient association of lipid raft-associated components with the macropinosomes harbouring *B. abortus*.

Cholesterol and GPI-anchored proteins are involved in VirB-dependent macropinocytosis

Based on the above results, the VirB-dependent delayed phagocytosis and macropinocytosis would be expected to be modulated by the lipid raft-associated components. To explore this possibility, we tested the effect of phosphatidylinositol phospholipase C (PI-PLC), a well-established approach to remove GPI-anchored molecules from the cell surface, or cholesterol-scavenging (β-cyclodextrin) or -binding (filipin and nystatin) drug treatment. PI-PLC greatly diminished the uptake of Ba600 (wild type) by bone marrow-derived macrophages as its concentration was increased (Fig. 7A), and delayed phagocytosis and macropinocytosis induced by Ba600 (wild type) were also inhibited (Figs 5C, D and 7C, D). Under the same conditions, non-PI-PLC did not block the uptake of Ba604 (Δ*virB4*) (Fig. 7A). Similar results were obtained for cholesterol-scavenging or -binding drug treatments. Filipin, β-cyclodextrin or nystatin greatly diminished the uptake of Ba600 (wild type) by macrophages as their concentration was increased (Fig. 8A–C). As expected, delayed phagocytosis and macropinocytosis were also inhibited by β-cyclodextrin treatment (Figs 8D and E), or filipin and nystatin (data not shown). However, internalization of Ba600 (wild type) was not inhibited completely by these drug treatments (27.4% at 2 U ml^{-1} PI-PLC, 28.1% at 5 mM β-cyclodextrin,

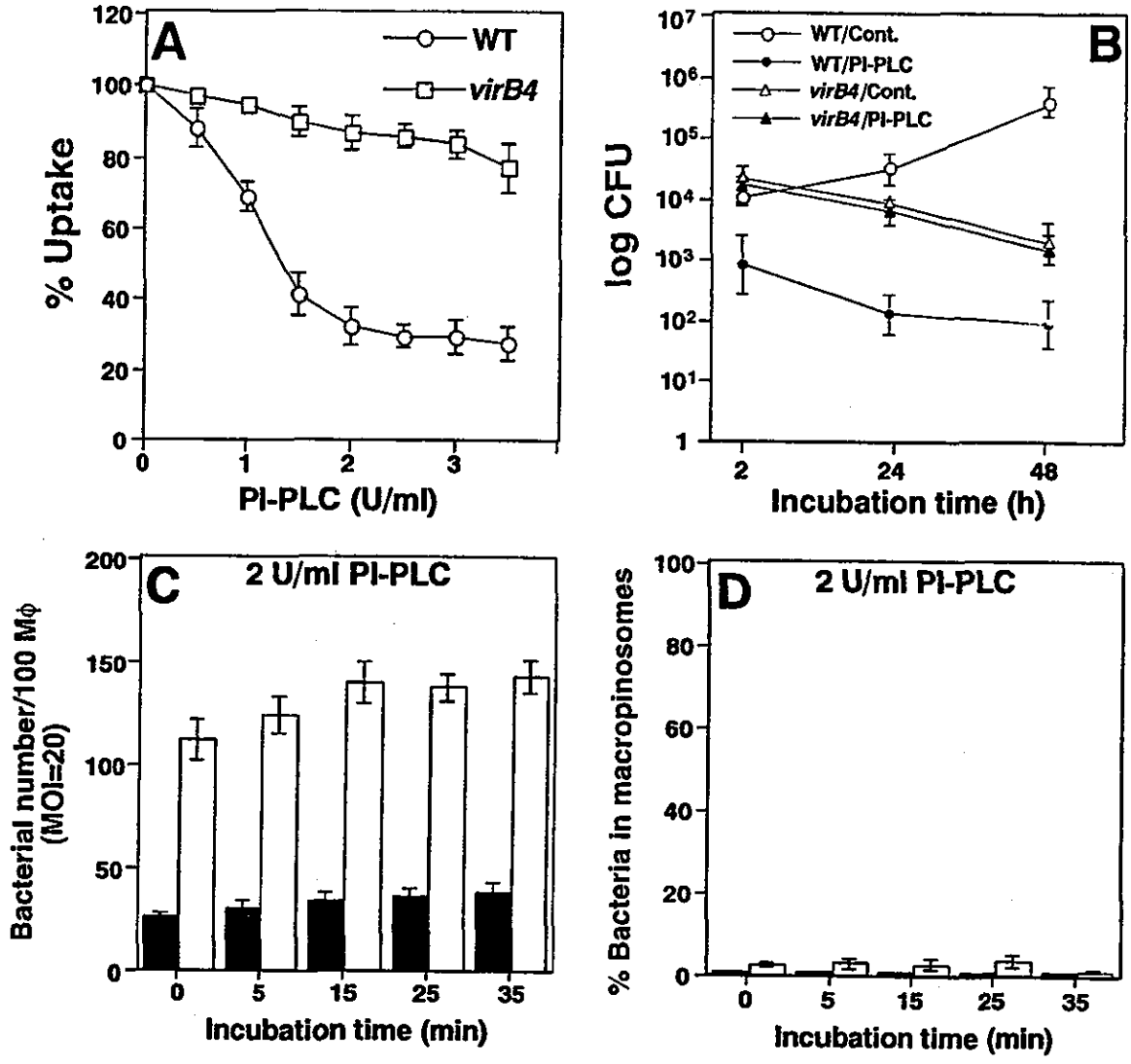

Fig. 7. PI-PLC inhibits delayed phagocytosis, macropinocytosis and intracellular replication of *B. abortus*.
A. Mouse bone marrow-derived macrophages were incubated with the noted concentration of PI-PLC for 1 h, and then Ba600 (wild type) or Ba604 (Δ*virB4*) were deposited onto the macrophages. After 15 min incubation at 37°C, cells were fixed and scored for internalized bacteria by fluorescence microscopy.
B. Intracellular replication of *B. abortus* in bone marrow-derived macrophages. Macrophages in the presence or absence of 2 U ml^{-1} PI-PLC were infected with Ba600 (wild type) or Ba604 (Δ*virB4*) as described in *Experimental procedures*. Data points and error bars represent the mean CFU of triplicate samples from a typical experiment (performed at least four times) and their standard deviation.
C and D. Bacteria were deposited onto macrophages in the presence of 2 U ml^{-1} PI-PLC and incubated at 37°C for the periods of time indicated. Uptake (C) or macropinosome formation (D) were quantitated as described (see *Experimental procedures*). One hundred macrophages were examined per coverslip. Black bars, Ba600 (wild type); open bars, Ba604 (Δ*virB4*). Data are the average of triplicate samples from three identical experiments, and the error bars represent the standard deviation.

25.2% at 1 μg ml^{-1} filipin, 21.7% at 30 μg ml^{-1} nystatin respectively) (Figs 7 and 8).

To determine whether the lipid raft-associated components play some role in bacterial replication in bone marrow-derived macrophages, macrophages were treated with PI-PLC or cholesterol-scavenging or -binding drugs and then infected with Ba600 (wild type). As reported previously (Watarai *et al.*, 2002), Ba600 (wild type) was able to replicate in macrophages without drug treatment. In contrast, Ba600 (wild type) failed to replicate in PI-PLC or cholesterol-scavenging or -binding drug-treated macrophages (Figs 7B and 8F). Under the same conditions, these drug treatments did not affect the intracellular growth of Ba604 (Δ*virB4*) (Figs 7B and 8G).

Discussion

In this study, we have shown that the uptake of *Brucella abortus* by mouse bone marrow-derived macrophages was unconventional in terms of both the entry process

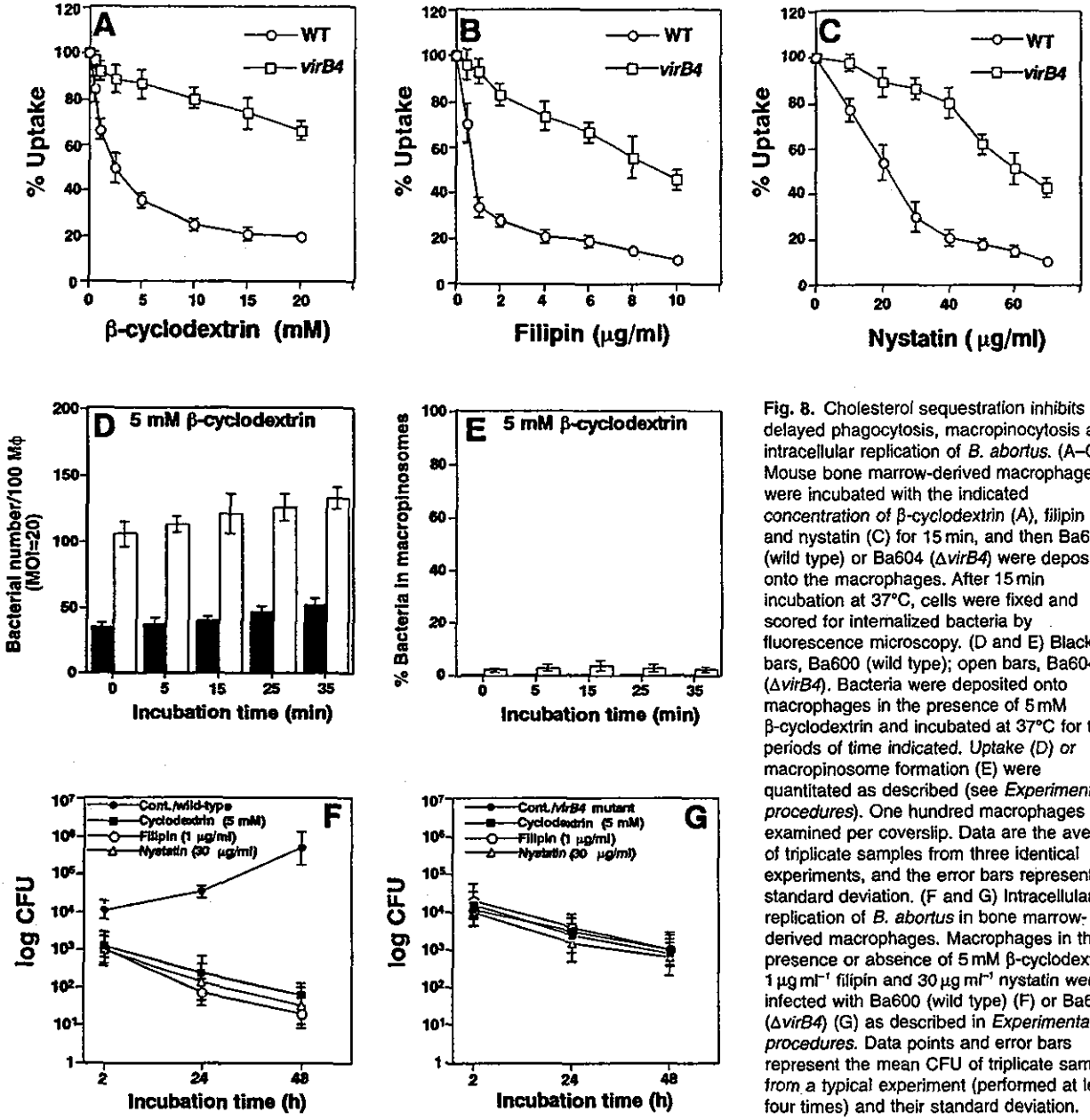

Fig. 8. Cholesterol sequestration inhibits delayed phagocytosis, macropinocytosis and intracellular replication of *B. abortus*. (A–C) Mouse bone marrow-derived macrophages were incubated with the indicated concentration of β-cyclodextrin (A), filipin (B) and nystatin (C) for 15 min, and then Ba600 (wild type) or Ba604 (Δ*virB4*) were deposited onto the macrophages. After 15 min incubation at 37°C, cells were fixed and scored for internalized bacteria by fluorescence microscopy. (D and E) Black bars, Ba600 (wild type); open bars, Ba604 (Δ*virB4*). Bacteria were deposited onto macrophages in the presence of 5 mM β-cyclodextrin and incubated at 37°C for the periods of time indicated. Uptake (D) or macropinosome formation (E) were quantitated as described (see *Experimental procedures*). One hundred macrophages were examined per coverslip. Data are the average of triplicate samples from three identical experiments, and the error bars represent the standard deviation. (F and G) Intracellular replication of *B. abortus* in bone marrow-derived macrophages. Macrophages in the presence or absence of 5 mM β-cyclodextrin, 1 μg ml^{-1} filipin and 30 μg ml^{-1} nystatin were infected with Ba600 (wild type) (F) or Ba604 (Δ*virB4*) (G) as described in *Experimental procedures*. Data points and error bars represent the mean CFU of triplicate samples from a typical experiment (performed at least four times) and their standard deviation.

and the morphology of the phagosome. These events were dependent on the presence of the VirB system. After contact of macrophages with *B. abortus*, the bacteria moved from the bacterial attachment site in a 'swimming' motion on the surface of the macrophage. The early events in phagocytosis by macrophages, especially the uptake of immunoglobulin- and complement-coated particles, are thought to occur by a zipper-like interaction between receptors and ligands. Zipper phagocytosis gives rise to the sequential and circumferential interaction between competent receptors on the surface of the macrophage and complementary ligands on the surface of the particle (Griffin *et al.*, 1975). However, non-zipper routes have been shown for microbial uptake into host cells. The uptake of *Legionella pneumophila*, *Borrelia burgdorferi* and *Leshmania* spp. occurs via coiling phagocytosis in which a single pseudopod wraps around the bacterium (Horwitz, 1984; Rittig *et al.*, 1998). In this study, we have presented data that *B. abortus* strains competent for replicative phagosome formation induce an uptake process that is morphologically distinct from that promoted by strains that have a defective VirB system, and this is apparently unrelated to zipper phagocytosis or coiling phagocytosis. This novel swimming internalization into the target macrophage continued for several minutes before enclosure within the macropinosome. Consistent

with this result, internalization of the wild-type strain was delayed and attained the same levels of internalization as the mutant strain only after 25 min incubation. With regards to delayed phagocytosis caused by the presence of the VirB system, previous work has demonstrated that internalization of *Helicobacter pylori* by macrophages is slower than that observed for other bacteria or non-pathogenic mutants (Allen *et al.*, 2000). As *H. pylori* appears to have a specific system for antagonizing phagocytosis (Ramarao *et al.*, 2000), the delayed phagocytosis may play different roles in the pathogenesis of these organisms.

Other non-zipper routes of microbial uptake have been reported. Internalization of *Salmonella typhimurium* by mouse bone marrow-derived macrophages is accompanied by macropinosome formation, and the persistence of these spacious phagosomes correlates with the ability of the microorganism to survive intracellular killing mechanisms (Alpuche-Aranda *et al.*, 1994). The spacious phagosomes could dilute toxic compounds, thus allowing *Salmonella* to initially survive. When combined with a delay in acidification of this phagosome, the bacterium may create a tolerable intracellular environment (Alpuche-Aranda *et al.*, 1994). In the case of *B. abortus*, macropinosomes were induced transiently and shrank rapidly, with the majority of vacuoles appearing tightly apposed against the bacterial surface within 20 min after their initial appearance (Fig. 2B). The swimming internalization with generalized membrane ruffling and macropinocytosis was observed within minutes of attachment to bacteria on the surface of the macrophage. Presumably, effector molecule(s) are translocated via the VirB system to the target cell during bacterial contact, initiating the process that leads to formation of the macropinosome. Opsonization enhanced the macropinosome formation by increasing affinity between *B. abortus* and macrophage, implying that effector molecule(s) were translocated into the target macrophage more efficiently.

Previous work reported the observation by electron microscopy of the intracellular transport of *B. abortus* and the kinetics of the fusion of phagosomes in J774 macrophage-like cell line with preformed lysosomes labelled with colloidal gold particles (Arenas *et al.*, 2000). In that study, phagosomes containing live *B. abortus* delayed fusion with lysosomes, and newly endocytosed material was not incorporated into these phagosomes. In this study, we tested the ability of wild-type strain and Δ*virB4* mutant to fuse with macropinosomes within bone marrow-derived macrophages. Consistent with previous work (Arenas *et al.*, 2000), macropinosomes harbouring wild-type strain resisted fusion with other macropinosomes in the macrophage. In contrast, phagosomes harbouring the mutant strain were able to fuse with TRDx preloaded macropinosomes after internalization. We also tested the ability of wild-type strain and Δ*virB4* mutant to target properly within macrophages. Bacterial phagosomes were scored for acquisition of the lysosomal glycoprotein LAMP-1, an abundant transmembrane protein found predominantly in late endosomes and lysosomes (Harter and Mellman, 1992; Chen *et al.*, 1988). Our results, together with previous evidence, indicate that *B. abortus* prevents phagosome-lysosome fusion after uptake by macrophages. In addition, more than 90% of the macropinosomes harbouring wild-type strain failed to colocalize with LAMP-1 in macrophages. These results led us to hypothesize that the formation of the VirB-dependent macropinosome involves a membrane sorting process.

As observed previously, aerolysin from *A. hydrophila*, which binds to GPI-anchored proteins on the cell surface (Abrami *et al.*, 1998; Wang *et al.*, 1999), affected to the replicative phagosomes harbouring *B. abortus* (Pizarro-Cerda *et al.*, 1998a). Treatment of infected cells with aerolysin caused vacuolation of the bacterial replication compartment in HeLa cells. We consistently found that aerolysin-labelled GPI-anchored proteins and CD48 are incorporated into macropinosomes harbouring the wild-type strain. We also found that lipid raft-associated components such as cholesterol and GM1 gangliosides were incorporated into macropinosomes harbouring *B. abortus*. Thus, formation of the *B. abortus* macropinosome may involve selective retention of plasma membrane proteins and exclusion of others. It has been reported that GPI-anchored proteins were included into apicomplexan *Toxoplasma gondii* and *Plasmodium falciparum* vacuoles (Mordue *et al.*, 1999; Lauer *et al.*, 2000). A similar process of selective lipid recruitment has been described during influenza viral budding from mammalian cells (Scheiffele *et al.*, 1999). In addition, Gatfield and Pieters (2000) reported that cholesterol was essential for uptake of *Mycobacterium bovis* by macrophages. Cholesterol accumulated at the site of *M. bovis* entry and depleting plasma membrane cholesterol specifically inhibited *M. bovis* uptake, and *M. bovis* displayed a high binding capacity for cholesterol. A recent study showed that more than 140 proteins associated with latex bead-containing phagosomes using a proteomic approach and lipid rafts enriched flotillin-1 also presented on phagosomes (Garin *et al.*, 2001). The intracellular parasite *Leshmania donovani* can actively inhibit the acquisition of flotillin-1-enriched lipid rafts by phagosomes and the maturation of these organelles (Dermine *et al.*, 2001). As lipid rafts are thought to be involved in signalling pathways in immune cells (Cherukuri *et al.*, 2001), it has been argued that raft-associated uptake processes may lead micoorganisms

into compartments that avoid fusion with the lysosomal network (Shin and Abraham, 2001). Indeed, macropinocytosis induced by *B. abortus* was inhibited by molecules that sequester cholesterol and PI-PLC, which removed GPI-anchored proteins from the macrophage surface. On the other hand, 21–28% of internalized *B. abortus* cells were observed under these drug treatments, but the internalized bacteria were not able to replicate in the macrophages. We consistently found that approximately 15% of internalized bacteria target improperly into a LAMP-1 positive compartment. These results suggest that there are other uptake pathways of *B. abortus* by macrophages, but replicative phagosome formation is necessary for the uptake pathway of VirB system-dependent macropinocytosis.

Both macropinosome formation and delayed phagocytosis rates, observed in this study, were documented recently with *Legionella pneumophila*, and macropinosomes harbouring *L. pneumophila* included in the lipid rafts-associated macromolecules (Watarai *et al.*, 2001a). *Legionella pneumophila* has the ability to modulate trafficking of the phagosomes in which they reside (Vogel and Isberg, 1999). *Legionella pneumophila* resides in a phagosome that restricts its fusion with host endosomes and lysosomes (Horwitz, 1983) and the intracellular fate of *L. pneumophila* is determined by the type IV transport system, Dot/Icm apparatus (Christie and Vogel, 2000). On the other hand, *B. abortus* contains the type IV transport system, VirB apparatus (Sieira *et al.*, 2000). Although the Dot/Icm system of *L. pneumophila* is unrelated to the VirB system of *B. abortus* from the DNA sequence data, it is thought that there are similarities between the internalization strategies of *B. abortus* and *L. pneumophila* from the functional similarities between Dot/Icm and VirB systems (Christie and Vogel, 2000). Therefore, we concluded that *B. abortus* altered the plasma membrane into a specialized organelle permissive for bacterial growth through the specific action of the VirB system during swimming on the macrophage surface with generalized membrane ruffling. Subsequently, macropinosomes were formed transiently with the selective incorporation of lipid raft-associated components, and replicative phagosomes were established.

Our findings provide a plausible explanation for the intracellular growth of *B. abortus* in macrophages. However, an effector molecule(s), which would be translocated into the target macrophage through the bacterial membrane via VirB system, remains unknown. The putative effector molecules or components of the VirB system may initially interact directly or indirectly with lipid raft-associated molecules after contact of macrophages with *B. abortus*. This possibility warrants further investigation.

Experimental Procedures

Regents

TRITC-dextran of molecular weight 155 000 (TRDx), filipin, phosphatidylinositol phospholipase C (PI-PLC), cycloheximide were obtained from Sigma (St Louis, MO). Nystatin and β-cyclodextrin were obtained from Wako Pure Chemical Industries (Tokyo, Japan). Cholera toxin B subunit (CTB)-biotin conjugate was obtained from List Biological Laboratories (Campbell, CA). Alexa Fluor 594-phalloidin, Alexa Fluor 594-streptavidin, Cascade blue-goat anti-rabbit IgG, Texas red-goat anti-rat IgG were obtained from Molecular Probes (Eugene, OR). Rhodamine-goat anti-rabbit IgG was obtained from ICN Phamaceuticals (Aurora, OH). Anti-*B. abortus* polyclonal rabbit serum was described previously (Watarai *et al.*, 2002). Anti-LAMP-1 rat monoclonal antibody 1D4B was obtained from the Developmental Studies Hybridoma Bank of the Department of Pharmacology and Molecular Sciences, Johns Hopkins University School of Medicine, Baltimore, MD, and the Department of Biology, University of Iowa, Iowa City, IA. Anti-mouse CD44 rat monoclonal antibody KM201 was obtained from Southern Biotechnology Associates (Birmingham, AL). Anti-mouse CD48 rat monoclonal antibody MRC OX-78 was obtained from Serotech (Oxford, UK).

Bacterial strains and media

All *B. abortus* derivatives were from 544 (ATCC23448), smooth virulent *B. abortus* biovar 1 strains. Ba598 (544 Δ*virB4*) has been described previously (Watarai *et al.*, 2002). *Brucella abortus* strains were maintained as frozen glycerol stocks and were cultured on *Brucella* broth (Becton Dickinson, Cockeysville, MD) or *Brucella* broth containing 15% agar. Kanamycin was used at 40 μg ml^{-1}.

The plasmid pMAW114 encoding green fluorescence protein (GFP) was constructed by cloning the *Bam*HI–*Bgl*II fragment from pQBI63 (GFP expression vector; TAKARA, Tokyo, Japan) into *Bam*HI and *Bgl*II-cleaved pBBR1MCS-2 (Kovach *et al.*, 1995). pMAW114 (GFP$^+$) was introduced into 544 (wild type) and Ba598 (Δ*virB4*), and the derivatives were designated Ba600 (wild-type GFP$^+$) and Ba604 (Δ*virB4* GFP$^+$) respectively.

Cell culture

Bone marrow-derived macrophages from female BALB/c mice were prepared as described (Watarai *et al.*, 2001b). After culturing in L-cell conditioned medium, the macrophages were replated for use by lifting cells in phosphate-buffered saline (PBS) on ice for 5–10 min, harvesting cells by centrifugation, and resuspending cells in RPMI 1640 containing 10% fetal bovine serum. The macrophages were seeded (2–3 × 10^5 per well) in 24-well tissue culture plates for all assays.

Time lapse video microscopy

Bone marrow-derived macrophages were plated in Laboratory-Tek Chambered coverglass (Nalge Nunc, Naperville, IL) and incubated overnight in RPMI 1640 containing 10% FBS at 37°C in 5% CO_2. Bacteria (2 × 10^6 ml^{-1}) were added to the chamber, which was then placed on a heated microscope stage and set to

37°C for observation, using an Olympus IX70 inverted phase microscope with 100× UPlanApo lens fitted with phase-contrast optics. The bacteria were allowed to pellet passively onto the macrophages, and images were captured over a 30 min period. If further observations were desired, new samples were prepared and the procedure was initiated again.

To capture images, the lens was focused on the upper surface of the macrophage. When bacteria began to appear within the focal plane of the image, the images were captured every 6 s using a cooled CCD camera (CoolSNAP; Roper Scientific, Trenton, NJ), and processed using Openlab software (Improvision, Lexington, MA) on a Power Macintosh G4 computer.

F-actin staining

Bacteria were deposited onto the macrophages by centrifugation at 150 *g* for 5 min at room temperature and were then incubated at 37°C for 5 min. Infected macrophages were fixed in periodate-lysine-paraformaldehyde (PLP) (McLean and Nakane, 1974) containing 5% sucrose for 1 h at 37°C. Samples were washed three times in PBS and wells were successively incubated three times for 5 min in blocking buffer (2% goat serum in PBS) at room temperature. Samples were stained with anti-*B. abortus* polyclonal rabbit serum diluted 1 : 1000 in blocking buffer to identify extracellular bacteria. After incubating for 1 h at 37°C, samples were washed three times for 5 min with blocking buffer, stained with Cascade blue-conjugated goat anti-rabbit IgG diluted 1:500 in blocking buffer, and incubated for 1 h at 37°C. Then, samples were permeabilized in 0.1% Triton X-100, washed three times with PBS and incubated with Alexa Fluor 594-phalloidin for 30 min at 37°C. After three washes with PBS, samples were placed in mounting medium (90% glycerol containing 1 mg ml^{-1} phenylenediamene in PBS, pH 9.0) and visualized by fluorescence microscopy.

Detection of intracellular bacteria and macropinosome formation by fluorescence microscopy

Brucella abortus strains were grown to $A_{600} = 3.2$ in *Brucella* broth and used to infect mouse bone marrow-derived macrophages for various lengths of time at an indicated multiplicity of infection (MOI). Bacteria in 250 µl of RPMI 1640 containing 1 mg ml^{-1} of TRDx were deposited onto the macrophages by centrifugation at 150 *g* for 5 min at room temperature, and were then incubated at 37°C, for 0 (no incubation), 5, 15, 25 and 35 min. Infected cells were fixed in PLP-sucrose for 1 h at 37°C and stained for extracellular bacteria as described above. Samples were washed three times and placed in mounting medium. One hundred macrophages were examined per coverslip to determine the total number of intracellular bacteria, macropinosome formation and the total number of bacteria within macropinsome. Macropinosome were defined as TRDx-labelled phagosomes in which detectable TRDx surrounding the bacteria was observed by fluorescence microscopy.

Opsonization

Bacteria ($2–3 \times 10^7$ ml^{-1}) were opsonized by incubation in PBS containing a 1:1000 dilution of anti-*B. abortus* polyclonal rabbit serum for 30 min at room temperature. Bacteria were washed twice with PBS before addition to macrophages. This opsonization procedure resulted in a greater than 10-fold enhancement in the amount of internalized bacteria for all strains observed.

Determination of efficiency of bacterial uptake by cultured macrophages

To determine the uptake of bacteria, mouse bone marrow-derived macrophages were infected with *B. abortus* as described in the previous section. After 0, 5, 15, 25 and 35 min incubation at 37°C, macrophages were washed once with medium and incubated with 30 µg ml^{-1} gentamicin for 30 min. Macrophages were then washed three times with fresh medium and lysed with distilled water. Colony-forming units (CFU) were determined by serial dilutions on *Brucella* plates. Percentage protection was determined by dividing the number of bacteria surviving the assay by the number of bacteria in the infectious inoculum, as determined by viable counts.

Determination of efficiency of intracellular growth of bacteria

Bacteria were deposited onto macrophages at a multiplicity of infection (MOI) of 20 by centrifugation at 150 *g* for 5 min at room temperature, and were then incubated at 37°C in 5% CO_2 for 1 h. The macrophages were then washed once with medium and incubated with 30 µg ml^{-1} gentamicin. At different time points, cells were washed and lysed with distilled water, and the number of bacteria was counted on plates of a suitable dilution.

Production and purification of aerolysin

Aerolysin was purified as described previously (Fujii *et al.*, 1998; Nomura *et al.*, 1999). The stock culture of *Aeromonas hydrophila* was grown overnight at 37°C in 5 ml of LB broth. The cells were collected by centrifugation and suspended in 5 ml of minimal salt medium containing 10 mM nitrilotriacetic acid (protease inhibitor; Tokyo Kasei, Tokyo, Japan) (Kozaki *et al.*, 1989). The suspension was transferred to 1 l of fresh minimal salt medium, followed by incubation for 48 h at 30°C without shaking. After cultivation, the cells in the medium were removed by centrifugation. The pH of the culture supernatant was adjusted to 4.0 with 2 N HCl. Six grams of SP-Sephadex C-25 (Pharmacia, Uppsala, Sweden), which was swollen and equilibrated with 10 mM citrate buffer (pH 5.0), were added to the culture supernatant. After gentle mixing at room temperature for 1 h, the gel was packed into a column. The column was washed with the citrate buffer to remove non-adsorbed materials, and adsorbed materials were eluted with a linear gradient of 0–0.3M NaCl in the same buffer. The fractions containing the aerolysin were collected and concentrated under vacuum. The concentrated solution was loaded onto a column of phenyl sepharose (Pharmacia) equilibrated with 10 mM phosphate buffer (pH 7.2) containing 5 mM EDTA and 2.5 mM EGTA. Non-adsorbed materials were washed out with the same buffer, and materials adsorbed to the column were eluted with a linear gradient of 0–50% ethylene glycol in the same buffer. Binding activity of aerolysin to GPI-anchored proteins was checked by using Intestine 407 cells, as described previously (Wang *et al.*, 1999).

Anti-aerolysin rabbit polyclonal serum was prepared as follows. Aliquots of 200 μg of the purified aerolysin were emulsified with complete Freund's adjuvant, and the emulsion was injected into the femoral muscle of a rabbit. At 2 week intervals, the same amount of purified aerolysin emulsified with incomplete Freund's adjuvant was also injected as boosters. Antiserum was obtained 2 weeks after the final injection. Sera were tested by Western blotting and stored at −80°C until use.

LAMP-1 staining

Infected macrophages were fixed in PLP-sucrose for 1 h at 37°C and stained for extracellular bacteria as described above. All antibody-probing steps were for 1 h at 37°C. Samples were washed three times in PBS for 5 min and then permeabilized at −20°C in methanol for 10 s. After incubating three times for 5 min with blocking buffer, samples were stained with anti-LAMP-1 rat monoclonal antibody 1D4B diluted 1:100 in blocking buffer (Swanson and Isberg, 1996). After washing three times for 5 min in blocking buffer, samples were stained simultaneously with Texas red-goat anti-rat IgG. Samples were placed in mounting medium and visualized by fluorescence microscopy. Intracellular bacteria were detected by GFP fluorescence and absence of staining with Cascade blue.

Colocalization of proteins with macropinosomes

To detect localization of GM1 gangliosides in macropinosomes, macrophage monolayers were incubated for 5 min with biotin-CTB (10 μg ml^{-1}), rinsed three times in RPMI and incubated with either Ba600 (wild type) and Ba604 (Δ*virB4*) for the indicated time periods at 37°C (Mordue *et al.*, 1999). The cells were washed once, fixed in PLP-sucrose and probed for extracellular bacteria, as above, before permeabilization in 0.05% saponin for 10 min at room temperature. After three washes with PBS and incubation in blocking buffer, the biotin-CTB was detected with Alexa Fluor 594-streptavidin (1:500 in blocking buffer). To detect glycosylphosphatidylinositol (GPI) linkages, samples fixed as above were permeabilized in methanol at −20°C for 10 s and probed with purified aerolysin (2.5 μg ml^{-1}) for 1 h at 37°C. Antibody-probing steps of aerolysin (1:1000), CD44 (1:100) and CD48 (1:25) were the same as in the previous section. To detect cholesterol, samples fixed as above were incubated in fluorescent cholesterol-binding drug filipin (50 mg ml^{-1}) for 2 h at room temperature (Mukherjee *et al.*, 1998). Extracellular bacteria were detected as above.

Drug treatment

PI-PLC treatment was performed in accordance with (Abrami *et al.* (1998). Briefly, mouse bone marrow-derived macrophages were incubated with RPMI 1640 containing 10 μg ml^{-1} cycloheximide and PI-PLC at various concentrations for 1 h at 37°C. After washing with medium containing cycloheximide, the macrophages were infected with bacteria as described in the previous section.

Mouse bone marrow-derived macrophages were exposed to β-cyclodextrin, filipin and nystatin at various concentrations for 15 min at 37°C. Macrophages were then infected with bacteria as described in the previous section.

© 2002 Blackwell Science Ltd, *Cellular Microbiology*, **4**, 341–355

Acknowledgements

We wish to thank Dr Ben Adler for critical suggestions on the manuscript. This work was supported, in part, by a grant from Grant-in-Aid for Scientific Research (12575029 and 13770129), Japan Society for the Promotion of Science.

References

Abrami, L., Fivaz, M., Glauser, P.E., Parton, R.G., and van der Goot, F.G. (1998) A pore-forming toxin interacts with a GPI-anchored protein and causes vacuolation of the endoplasmic reticulum. *J Cell Biol* **140:** 525–540.

Acha, P., and Szylres, B. (1980) *Zoonoses and Communicable Diseases Common to Man and Animals.* Washington, DC: Pan American Health Organization, pp. 28–45.

Allen, L.A., Schlesinger, L.S., and Kang, B. (2000) Virulent strains of *Helicobacter pylori* demonstrate delayed phagocytosis and stimulate homotypic phagosome fusion in macrophages. *J Exp Med* **191:** 115–128.

Alpuche-Aranda, C.M., Berthiaume, E.P., Mock, B., Swanson, J.A., and Miller, S.I. (1994) *Salmonella* stimulate macropinocytosis and persist within spacious phagosomes. *J Exp Med* **179:** 601–608.

Arenas, G.N., Staskevich, A.S., Aballay, A., and Mayorga, L.S. (2000) Intracellular trafficking of *Brucella abortus* J774 macrophages. *Infect Immun* **68:** 4255–4263.

Baldwin, C.L., and Winter, A.J. (1994) Macrophages and *Brucella*. *Immunol Ser* **60:** 363–380.

Bourdet-Sicard, R., Egile, C., Sansonetti, P.J., and Tran Van Nhieu, G. (2000) Diversion of cytoskeletal processes by *Shigella* during invasion of epithelial cells. *Microbes Infect* **2:** 813–819.

Chen, J.W., Cha, Y., Yuksel, K.U., Gracy, R.W., and August, J.T. (1988) Isolation and Sequencing of a cDNA Clone Encoding Lysosomal Membrane Glycoprotein Mouse LAMP-1. *J Biol Chem* **263:** 8754–8758.

Cherukuri, A., Dykstra, M., and Pierce, S.K. (2001) Floating the Raft Hypothesis. Lipid Rafts Play a Role in Immune Cell Activation. *Immunity* **14:** 657–660.

Christie, P.J., and Vogel, J.P. (2000) Bacterial type IV secretion: conjugation systems adapted to deliver effector molecules to host cells. *Trend Microbiol* **8:** 354–360.

Comerci, D.J., Martinez-Lorenzo, M.J., Sieira, R., Gorvel, J., and Ugalde, R.A. (2001) Essential role of the VirB machinery in the maturation of the *Brucella abortus*-containing vacuole. *Cell Microbiol* **3:** 159–168.

Covacci, A., Telford, J.L., Del Giudice, G., Parsonnet, J., and Rappuoli, R. (1999) *Helicobacter pylori* virulence and genetic geography. *Science* **284:** 1328–1333.

Dermine, J.-F., Duclos, S., Garin, J., St-Louis, F., Rea, S., Parton, R.G., and Desjardins, M. (2001) Flotillin-1-enriched lipid raft domains accumulate on maturing phagosomes. *J Biol Chem* **276:** 18507–18512.

Emst, J.D. (2000) Bacterial inhibition of phagocytosis. *Cell Microbiol* **2:** 379–386.

Fujii, Y., Nomura, T., Kanzawa, H., Kameyama, M., Yamanaka, H., Akita, M. *et al.* (1998) Purification and characterization of enterotoxin produced by *Aeromonas sobria*. *Microbiol Immunol* **42:** 703–714.

Galan, J.E. (2000) Alternative strategies for becoming an insider: lessons from the bacterial world. *Cell* **103:** 363–366.

Garin, J., Diez, R., Kieffer, S., Dermine, J.-F., Duclos, S., Gagnon, E., Sadoul, R., Rondeau, C., and Desjardins, M. (2001) The

phagosome proteome: insight into phagosome function. *J Cell Biol* **152:** 165–180.

Gatfield, J., and Pieters, J. (2000) Essential role for cholesterol in entry of mycobacteria into macrophages. *Science* **288:** 1647–1650.

Griffin, F.M., Griffin, J.A., Leider, J., E., and Silverstein, S.C. (1975) Studies on the mechanism of phagocytosis. I. Requirements for circumferential attachment of particle-bound ligands to specific receptors on the macrophage plasma membrane. *J Exp Med* **142:** 1263–1282.

Harter, C., and Mellman, I. (1992) Transport of the lysosomal membrane glycoprotein lgp120 (lgp-A) to lysosomes does not require appearance on the plasma membrane. *J Cell Biol* **177:** 311–325.

Horwitz, M.A. (1983) The Legionnaires' disease bacterium (*Legionella pneumophila*) inhibits phagosome-lysosome fusion in human monocytes. *J Exp Med* **158:** 1319–1331.

Horwitz, M.A. (1984) Phagocytosis of the Legionnaires' disease bacterium (*Legionella pneumophila*) occurs by a novel mechnism: engulfment within a pseudopod coil. *Cell* **36:** 27–33.

Isberg, R.R. (1996) Uptake of enteropathogenic *Yersinia* by mammalian cells. *Curr Topics Microbiol Immunol* **209:** 1–24.

Kotob, S.I., Hausman, S.Z., and Burns, D.L. (1995) Localization of the promoter for the *ptl* genes of *Bordetella pertussis*, which encode proteins essential for secretion of pertussis toxin. *Infect Immun* **63:** 3227–3230.

Kovach, M.E., Elzer, P.H., Hill, D.S., Robertson, G.T., Farris, M.A., Roop, R.M., and Peterson, K.M. (1995) Four new derivatives of the broad-host-range cloning vector pBBR1MCS, carrying different antibiotic-resistance cassettes. *Gene* **166:** 175–176.

Kozaki, S., Asao, T., Kamata, Y., and Dakaguchi, G. (1989) Characterization of *Aeromonas sobria* hemolysin by use of monoclonal antibodies against *Aeromonas hydrophila* hemolysins. *J Clin Microbiol* **27:** 1782–1786.

Kuldau, G.A., De Vos, G., Owen, J., McCaffrey, G., and Zambryski, P. (1990) The *virB* operon of *Agrobacterium tumefaciens* pTiC58 encodes 11 open reading frames. *Mol Gen Genet* **221:** 256–266.

Lauer, S., VanWye, J., Harrison, T., McManus, H., Samuel, B.U., Hiller, N.L. *et al.* (2000) Vacuolar uptake of host components, and a role for cholesterol and sphingomyelin in malarial infection. *EMBO J* **19:** 3556–3564.

Lecuit, M., Dramsi, S., Gottardi, C., Fedor-Chaiken, M., Gumbiner, B., and Cossart, P. (1999) A single amino acid in E-cadherin responsible for host specificity towards the human pathogen *Listeria monocytogenes*. *EMBO J* **18:** 3956–3963.

Lopes, M.F., Freire-d., e-Lima, C.G., and DosReis, G.A. (2000) The macrophage haunted by cell ghosts: a pathogen grows. *Immunol Today* **21:** 489–494.

McLean, I.W., and Nakane, P.K. (1974) Periodate-lysine-paraformaldehyde fixative: a new fixative for immunoelectron microscopy. *J Histochem Cytochem* **22:** 1077–1083.

Méresse, S., Steele-Mortimer, O., Moreno, E., Desjardins, M., Finlay, B., and Gorvel, J. (1999) Controlling the maturation of pathogen-containing vacuoles: a matter of life and death. *Nat Cell Biol* **1:** 183–188.

Mordue, D.G., Desai, N., Dustin, M., and Sibley, L.D. (1999) Invasion by *Toxoplasma gondii* establishes a moving junction that selectively excludes host cell plasma membrane proteins on the basis of their membrane anchoring. *J Exp Med* **190:** 1783–1792.

Mukherjee, S., Zha, X., Tabas, I., and Maxfield, F.R. (1998) Cholesterol distribution in living cells: fluorescence imaging using dehydroergosterol as a fluorescent cholesterol analog. *Biophys J* **75:** 1915–1925.

Nomura, T., Fujii, Y., and Okamoto, K. (1999) Secretion of hemolysin of *Aeromonas sobria* as protoxin and contribution of the propeptide region removed from the protoxin to the proteolytic stability of the toxin. *Microbiol Immunol* **43:** 29–38.

O'Callaghan, D., Cazevieille, C., Allardet-Servent, A., Boschiroli, M.L., Bourg, G., Foulongne, V. *et al.* (1999) A homologue of the *Agrobacterium tumefaciens* VirB and *Bordetella pertussis* Ptl type IV secretion systems is essential for intracellular survival of *Brucella suis*. *Mol Microiol* **33:** 1210–1220.

Pizarro-Cerda, J., Méresse, S., Parton, R.G., van der Goot, G., Sola-Landa, A., Lopez-Goni, I. *et al.* (1998a) *Brucella abortus* transits through the autophagic pathway and replicates in the endoplasmic reticulum of nonprofessional phagocytes. *Infect Immun* **66:** 5711–5724.

Pizarro-Cerda, J., Moreno, E., Sanguedolce, V., Mege, J.L., and Gorvel, J.P. (1998b) Virulent *Brucella abortus* prevents lysosome fusion and is distributed within autophagosome-like compartments. *Infect Immun* **66:** 2387–2392.

Pohlman, R.F., Genetti, H.D., and Winans, S.C. (1994) Common ancestry between IncN conjugal transfer genes and macromolecular export systems of plant and animal pathogens. *Mol Microbiol* **14:** 655–668.

Ramarao, N., Gray-Owen, S.D., Backert, S., and Meyer, T.F. (2000) *Helicobacter pylori* inhibits phagocytosis by professional phagocytes involving type IV secretion components. *Mol Microbiol* **37:** 1389–1404.

Rittig, M.G., Burmester, G.R., and Krause, A. (1998) Coiling phagocytosis: when the zipper jams, the cup is deformed. *Trends Microbiol* **6:** 384–388.

Sangari, F.J., and Aguero, J. (1996) Molecular basis of *Brucella* pathogenicity: an update. *Microbiologia* **12:** 207–218.

Scheiffele, P., Rietveld, A., Wilk, T., and Simons, K. (1999) Influenza viruses select ordered lipid domains during budding from the plasma membrane. *J Biol Chem* **274:** 2038–2044.

Segal, G., Purcell, M., and Shuman, H.A. (1998) Host cell killing and bacterial conjugation require overlapping sets of genes within a 22-kb region of the *Legionella pneumophila* genome. *Proc Natl Acad Sci USA* **95:** 1669–1674.

Shin, J.S., and Abraham, S.N. (2001) Review Article: Co-option of endocytic functions of cellular caveolae by pathogens. *Immunology* **102:** 2–7.

Sieira, R., Comerci, D.J., Sanchez, D.O., and Ugalde, R.A. (2000) A homologue of an operon required for DNA transfer in *Agrobacterium tumefaciens* is required in *Brucella abortus* for virulence and intracellular multiplication. *J Bacteriol* **182:** 4849–4855.

Sinai, A.P., and Joiner, K.A. (1997) Safe haven: the cell biology of nonfusogenic pathogen vacuoles. *Annu Rev Microbiol* **51:** 415–462.

Stachel, S.E., and Nester, E.W. (1986) The genetic and transcriptional organization of the *vir* region of the A6 Ti plasmid of *Agrobacterium tumefaciens*. *EMBO J* **5:** 1445–1454.

Swanson, J.A. (1989) Phorbol esters stimulate macropinocytosis and solute flow through macrophages. *J Cell Sci* **94:** 135–142.

Swanson, M.S., and Isberg, R.R. (1996) Identification of *Legionella pneumophila* mutants that have aberrant intracellular fates. *Infect Immun* **64:** 2585–2594.

Vogel, J.P., and Isberg, R.R. (1999) Cell Biology of *Legionella pneumophila*. *Curr Opin Microbiol* **2:** 30–34.

Vogel, J.P., Andrews, H.L., Wong, S.K., and Isberg, R.R. (1998) Conjugative transfer by the virulence system of *Legionella pneumophila*. *Science* **279:** 873–876.

Wang, A.P., Wada, A., Yahiro, K., Nomura, T., Fujii, Y., Okamoto, K. *et al.* (1999) Identification and characterization of the *Aeromonas sobria* hemolysin glycoprotein receptor on intestine 407 cells. *Microb Pathog* **27:** 215–221.

Watarai, M., Derre, I., Kirby, J., Growney, J.D., Dietrich, W.F., and Isberg, R.R. (2001a) *Legionella pneumophila* is internalized by a macropinocytotic uptake pathway controlled by the Dot/Icm system and the mouse *Lgn1* locus. *J Exp Med* **194:** 1081–1095.

Watarai, M., Andrews, H.L., and Isberg, R.R. (2001b) Formation of a fibrous structure on the surface of *Legionella pneumophila* associated with exposure of DotH and DotO proteins after intracellular growth. *Mol Microbiol* **39:** 313–329.

Watarai, M., Makino, S., and Shirahata, T. (2002) An essential virulence protein of Brucella abortus, VirB4, requires an intact nucleoside triphosphate-binding domain. *Microbiology* **148:** 1439–1446.

Weiss, A.A., Johnson, F.D., and Burns, D.L. (1993) Molecular characterization of an operon required for pertussis toxin secretion. *Proc Natl Acad Sci USA* **90:** 2970–2974.

Winans, S.C., and Walker, G.C. (1985) Conjugal transfer system of the IncN plasmid pKM101. *J Bacteriol* **161:** 402–410.

Zavala, I., Nava, A., Guerra, J., and Quiros, C. (1994) Brucellosis. *Infect Dis Clin N Am* **8:** 225–241.

Effect of the Lower Molecular Capsule Released from the Cell Surface of *Bacillus anthracis* on the Pathogenesis of Anthrax

Sou-ichi Makino,[1] Masahisa Watarai,[1] Hyeng-il Cheun,[1] Toshikazu Shirahata,[1] and Ikuo Uchida[2]

[1]*Department of Veterinary Microbiology, Obihiro University of Agriculture and Veterinary Medicine, Obihiro, Hokkaido, and* [2]*Hokkaido Branch, National Institute of Animal Health, Sapporo, Hokkaido, Japan*

Bacillus anthracis **enters the body as an endospore, and encapsulation and toxin production occur after germination. Capsule is proposed to be an antiphagocytic factor, and toxin induces cytokine production for systemic shock. The *dep* gene, adjacent to the *cap* region for the encapsulation, degrades the high–molecular weight capsule (H-capsule) to the lower–molecular weight capsule (L-capsule), which releases into the culture supernatant. This study analyzed the biological function of the *cap-dep* region. The *dep* null mutant Sm-1, which formed H-capsule but not L-capsule, was avirulent. However, Sm-1 with an intact *dep* gene or with purified L-capsule recovered its pathogenicity. Sm-1 was subjected to phagocytosis by macrophages more easily than its parent strain, Sm, in vitro; in vivo, it cleared without L-capsule and grew well with L-capsule, which suggests that L-capsule is essential for in vivo multiplication. Moreover, a new name, *capD*, might be appropriate, because of the part of the *cap* operon involved in both polymerization and depolymerization of the capsule.**

Bacillus anthracis causes anthrax, a disease of domestic and wild animals. Humans can also become infected through contact with diseased animals. It is well established that *B. anthracis* has 2 major virulence factors, a capsule composed of a homopolymer of D-glutamic acid and a tripartite protein exotoxin consisting of protective antigen, edema factor, and lethal factor [1–4]. The toxin and capsule are encoded by separate plasmids having molecular masses of 110 and 60 mDa, respectively [5–7].

Anthrax is initiated by introduction into the body of *B. anthracis* endospores [8], which then efficiently and rapidly undergo phagocytosis [9]. After spore germination and multiplication within macrophages, vegetative bacilli kill the macrophages and are released into the bloodstream where they replicate extracellularly and reach high numbers [8]. Finally, the systemic form of anthrax, which is nearly always fatal, may be generated [10–12].

The vegetative bacilli respond to host signals of body temperature and CO_2 levels, resulting in transcriptional activation of capsule and toxin genes. This activation, detected when cells were grown in media containing elevated bicarbonate in vitro [13–17], involves 2 genes, *atxA* for toxin production and *acpA* for encapsulation, which are located on the 110- and 60-mDa plasmids, respectively [7, 18–20]. Moreover, it was reported that the *atxA* gene also positively regulated encapsulation [17], which means that both virulence factors were expressed cooperatively in vivo.

The vegetative bacilli produce toxin, which induces high-level production of cytokines, mainly interleukin-1, resulting in systemic shock and death [12]. On the other hand, encapsulation has been proposed to inhibit host defense through macrophage-induced inhibition of phagocytosis of the vegetative bacilli.

Although the *cap* region containing *capA*, *capB*, and *capC* on a 60-mDa plasmid is essential for encapsulation [16], we have reported an additional gene, *dep* [21]. The *dep* gene product degraded the high–molecular weight capsule (H-capsule) of >100 kDa, which is first polymerized on the bacterial cell surface in vivo, to the lower–molecular weight capsule (L-capsule) of <14 kDa, resulting in the release of capsule from the bacterial cell surface into the culture supernatant. Although the biological function of the *dep* gene is unknown, it has been proposed that the depolymerization process may be an essential host defense mechanism. The *cap-dep* gene cluster may be coexpressed in vivo, which suggests that the depolymerization is an essential process in the pathogenesis of anthrax, especially the extracellular growth of *B. anthracis*. In this study, we analyzed the biological function of the *cap-dep* region by examining the expression of these genes and by experimentally infecting mice with the *dep* null mutant, to investigate the escape mechanisms of *B. anthracis* from host defense mechanisms.

Received 14 January 2002; revised 14 March 2002; electronically published 27 June 2002.

Guidelines approved by the Obihiro University of Agriculture and Veterinary Medicine for animal care and use were followed in the animal studies.

Financial support: Japanese Ministry of Education, Science, and Culture (grant 10877046); Japanese Ministry of Health and Welfare (Research on Emerging and Re-emerging Infectious Diseases). H.-I.C. was a research scientist of the Japan Health Sciences Foundation.

Reprints or correspondence: Dr. Sou-ichi Makino, Dept. of Veterinary Microbiology, Obihiro University of Agriculture and Veterinary Medicine, Inada-cho, Obihiro, Hokkaido 080-8555, Japan (smakino@obihiro.ac.jp).

The Journal of Infectious Diseases 2002; 186:227–33

0022-1899/2002/18602-0011$15.00

Materials and Methods

Bacterial strains and plasmid. *B. anthracis* Sm, a spontaneous streptomycin-resistant strain of the Pasteur II strain carrying capsule and toxin plasmids [21], was used as the parent strain in this study. Also used were Sm-1, a *dep* null mutant of Sm; Sm-2, which is Sm-1 carrying pDEP10, a plasmid with an intact *dep* gene [21] that was constructed in pHY300PLK (Takara); and Sm-3, a capsule-negative mutant (*cap* mutant) of Sm.

Isolation of L-capsule. L-capsule was purified from bacterial culture supernatant, as described elsewhere [17, 21]. In brief, *B. anthracis* strain Sm was grown without shaking in 200 mL of NBY broth [5] containing 0.8% $NaHCO_3$ for 24 h at 37°C in an atmosphere containing 20% CO_2. After centrifugation, the supernatant was filtered through a 0.45-mm filter to remove bacterial cells, followed by the addition of 3 vol of ethanol. After centrifugation, the precipitate was resuspended in sterile distilled water, and the ethanol precipitation was repeated 3 times. The final precipitate was suspended in 1 mL of sterile PBS, autoclaved for 30 min at 121°C to destroy enzymatic activities in the suspension, and then used as capsular substance for further experiments. At the same time, the precipitate was hydrolyzed by heating for 120 min at 110°C in 2 *N* HCl, followed by dialysis. For some experiments, 100 μL of DNase (1 mg/mL; Pharmacia) or 10 μL of RNase (10 mg/mL; Sigma) was added to 100 μg of the capsular substance, followed by incubation for 60 min at 37°C, autoclaving for 30 min to destroy enzyme activity, and dialysis against sterile PBS overnight. In some cases, L-capsule was pretreated with 100 μL of fresh normal mice serum for 30 min at 37°C before infection, and the mixture was used for the infection experiments. As the control, heat-inactivated serum also was used.

Infection experiments. Female 6-week-old ICR mice (CLEA Japan) were used for infection experiments. Bacterial cells were grown in Luria broth for 16 h at 37°C with shaking, and ~10^6 cells were injected intraperitoneally into mice (n = 15 mice). At 6 and 24 h postinfection, 2 mL of sterile PBS was intraperitoneally injected into the abdominal cavities of all infected mice, followed by thorough mixing, and each 0.2 mL of the abdominal wash was collected, by use of a 1.0-mL syringe, for microscopic and microbiologic detection of *B. anthracis* cells in the samples. Simultaneously, at 24 h postinfection, 5 mice were killed, spleen and liver were removed and were homogenized in 1.0 mL of PBS per 100 mg of organ, and each 100 μL of the suspension was spread on Luria agar plates. The remaining 10 mice were observed for 14 days.

Infection assay of macrophage. Bone marrow–derived macrophages from female BALB/c mice (CLEA Japan) were prepared as described elsewhere [22]. After culturing in L cell–conditioned medium [22], the macrophages were replated for use by lifting cells in PBS onto ice for 5–10 min, harvesting cells by centrifugation, and resuspending cells in RPMI 1640 medium (Sigma) containing 10% fetal bovine serum (Sigma). The macrophages were seeded (2–3 × 10^5 cells/well) in 24-well tissue culture plates. *B. anthracis* strains were grown to A_{600} = 1.2 in Luria broth and were used to infect macrophages at an MOI of 20. Phagocytosis was allowed to proceed for 2 h at 37°C in an atmosphere containing 5% CO_2. After 3 washings with PBS, the culture medium was replaced with RPMI 1640 medium containing 30 μg/mL of gentamicin, and then the cells were incubated to eliminate noninternalized bacteria for 1 h at 37°C. Infected cells were fixed in 4.0% paraformaldehyde for 30 min at room temperature, after which samples were permeabilized in 0.1% Triton X-100 for 30 min at room temperature. Samples were washed 3 times in PBS and were incubated with anti–*B. anthracis* polyclonal rabbit serum diluted 1:500 in blocking buffer (2% goat serum in PBS) for 1 h at 37°C. Samples then were washed 3 times for 5 min with blocking buffer and were incubated for 1 h at 37°C with fluorescein isothiocyanate–conjugated goat anti–rabbit IgG (Sigma) diluted 1:500 in blocking buffer. Samples were washed 3 times and mounted in mounting medium (90% glycerol containing 1 mg/mL phenylenediamine in PBS). The specimens were analyzed by using a fluorescence microscope (Olympus), and images were collected by using a cooled slow-scan CCD camera (Coolsnap; Photometrics) and were processed by using Coolsnap imaging software.

Northern hybridization. Total RNA was purified from *B. anthracis,* as described elsewhere [23]. Each 8 μg of purified RNA samples was electrophoresed in 1.0% agarose gels containing 3-(*N*-morpholine) propane sulfonic acid buffer and formaldehyde, followed by transfer to nylon membranes for northern hybridization using DNA probes labeled with [^{32}P] γ-dTP (Amersham).

Results

Virulence of the dep *null mutant.* A *dep* null mutant, Sm-1, formed H-capsule on its surface at the same level as the parent strain, Sm, but no L-capsule was detected in culture supernatant [21]. To study the biological significance of L-capsule, the pathogenicity of Sm-1 for mice was tested. All mice infected with Sm and Sm-2 (Sm-1 carrying an intact *dep* gene [21]) died within 14 days (mean times, 1.7 and 2.0 days, respectively), whereas all mice infected with Sm-1 survived for 14 days. In addition, at 6 and 24 h postinfection, *B. anthracis* cells were microscopically and microbiologically detected in the abdominal washings from all mice infected with Sm and Sm-2 but not in those from any mice infected with Sm-1 (table 1). At 24 h postinfection, *B. anthracis* was also recovered from spleen and liver of all mice infected with Sm and Sm-2 but not from those of mice infected with Sm-1 (table 1). These data show that the *dep* mutant was immediately and completely eliminated in the abdominal cavity but that the parent strain could grow explosively in mice, leading to sepsis. Simultaneously, the *dep* mutant produced toxin at the same level as the parent strain when analyzed by Western blot, using antiserum raised against protective antigen (figure 1). These results show that the *dep* null mutant is avirulent and that the *dep* gene is essential for the virulence of *B. anthracis* in mice.

Role of L-capsule against host defense mechanisms. Since the *dep* gene was essential for the degradation of H-capsule to L-capsule [21], L-capsule might be associated with the pathogenicity of *B. anthracis*. Thus, 10 μg of L-capsule, purified from the culture supernatant of the parent strain, was mixed with 10^6 cells of the *dep* mutant just before intraperitoneal injection into mice. At 6 and 24 h postinfection, *B. anthracis* cells were microscopically and microbiologically detected in abdominal

Table 1. Virulence of *Bacillus anthracis* for mice.

	Culture supernatant			Mice				
							Bacterial detection[b]	
B. anthracis strain	Added	Origin	Pretreatment	No. of survivors after 14 days (n = 10)	Mean time to death, days	Bacterial isolation after 24 h (n = 5)[a]	After 6 h	After 24 h
Sm	No	—	ND	0	1.7	+	+	+
Sm-1	No	—	ND	10	—	−	−	−
Sm-2	No	—	ND	0	2.0	+	+	+
Sm-1	Yes	Sm (L-capsule)	ND	1	3.1	+	+	+
Sm-1	Yes	Sm-1	ND	10	—	−	−	−
Sm-1	Yes	Sm (L-capsule)	HCl heating	10	—	−	−	−
Sm-1	Yes	Sm (L-capsule)	DNase or RNase	1	3.5	+	+	+
Sm-1	Yes	Sm (L-capsule)	Normal serum	9	1.0	+[c]	−	−
Sm-1	Yes	Sm (L-capsule)	Heat-inactivated serum	2	3.5	+	−	−
—	Yes	Sm (L-capsule)	ND	10	—	−	−	−

NOTE. Bacterial cell detection was done intraperitoneally. —, Unknown; ND, not done.

[a] +, All cultures yielded confluent growth of *B. anthracis;* −, no colonies were formed on the plates.

[b] +, *B. anthracis* cells were observed microscopically in macrophages from all mice; −, *B. anthracis* cells were not observed in macrophages from all mice.

[c] *B. anthracis* cells were isolated from only 1 mouse, which died at 1 day postinfection.

washings from all mice (table 1). In addition, 9 of the 10 mice infected with the mixture died within 14 days (mean time, 3.1 days), and confluent growth of *B. anthracis* was detected in the organs of all mice at 24 h postinfection (table 1). To avoid the possibility that DNA uptake [24] might be responsible for the complementation observed, 10 μg of L-capsule pretreated with DNase or RNase was mixed with Sm-1 for the infection experiments, but the results were almost the same as those with untreated capsule (table 1). However, when L-capsule was hydrolyzed by heating in 2 *N* HCl, no bacteria were isolated from the mice (table 1). In addition, mice receiving only L-capsule survived, and no bacterial cells were detected in the organs; the concentrate purified from the culture supernatant of the capsule-negative mutant, Sm-3, also could not complement (table 1), showing that L-capsule inhibited the immediate elimination of the *dep* mutant in vivo. Therefore, we concluded that L-capsule exogenously complemented the loss of pathogenicity of Sm-1 for mice and that the production of L-capsule was essential for the pathogenicity of *B. anthracis*. However, when Sm-1 was mixed with L-capsule prereacted with heat-inactivated normal mouse serum at 37°C for 30 min before infection of mice, it regained its infectivity, but when the capsule was prereacted with fresh normal mouse serum, its infectivity was lost (table 1).

dep *Mutant increased uptake by macrophages.* On the basis of the observation described above, we reasoned that surface-exposed capsule might be involved in bacterial uptake by macrophages. To determine the rate of internalization, *B. anthracis* was added to macrophage monolayers. The number of intracellular bacteria was then determined by immunostaining after a 3-h infection (figure 2*A*–2*C*). For the parent strain, 75% of the infected macrophages contained only 1–5 bacteria (figure 2*G*). For the *dep* mutant, nearly 60% of the infected macrophages contained >15 bacteria; only rarely did a macrophage contain a single bacterium (figure 2*G*). To determine the efficiency of infection, we also scored the number of infected macrophages, per 300, that contained >1 bacterium. The number of macrophages infected by the *dep* mutant was close to 2 times greater than that infected by the parent strain (data not shown). However, when the *dep* mutant was mixed with L-capsule and infected macrophages, the efficiency of infection by the mixture was almost the same as that of infection by the *dep* mutant (figure 2*C* and 2*G*). These results indicated that the *dep* phenotype of *B. anthracis* would be involved in uptake by macrophages but that L-capsule could not inhibit uptake by macrophages in vitro.

Molecular analysis of the cap-dep *region.* As described elsewhere, *capB, capC,* and *capA* in the *cap* region and *dep* were transcribed in the same orientation, with spacing between the genes of only 10–30 bp [18, 25], which suggests that the *cap-dep* region may constitute a single transcriptional unit (figure 3*A*). In this case, the expression of *dep* should be induced in the pres-

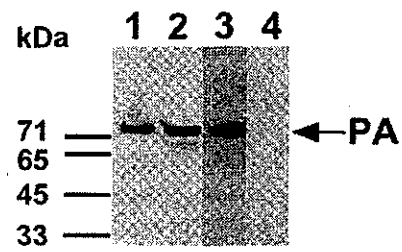

Figure 1. Western blot analysis using antiserum raised against protective antigen (PA). *Lane 1, Bacillus anthracis* Sm; *lane 2, B. anthracis* Sm-1; *lane 3,* purified PA. Bacterial cells were grown on NBY agar plates [5] for 24 h at 37°C in an atmosphere containing 20% CO_2, and identical bacterial cell nos. were used for the experiments. Molecular marker position (kDa) is shown *(upper left),* and PA protein is indicated *(arrow).*

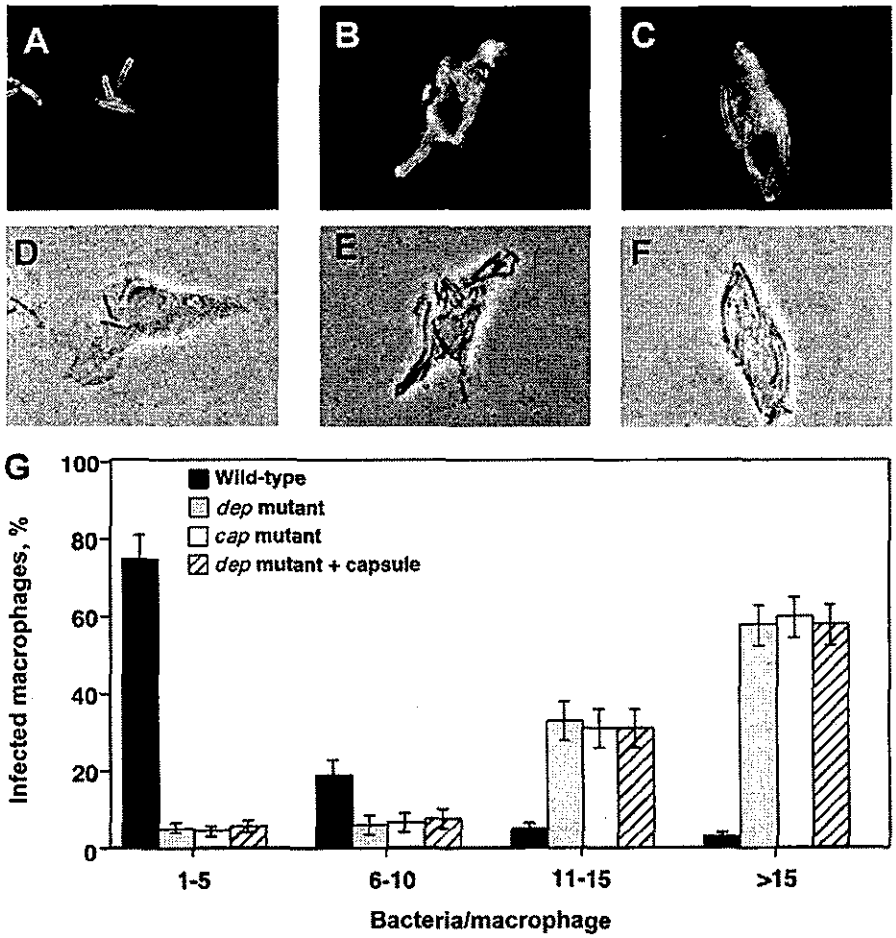

Figure 2. Immunofluorescence staining and phenotype of internalized *Bacillus anthracis*. Wild-type *B. anthracis (A* and *D)* or *dep* mutant *(B* and *E)* or *dep* mutant with L-capsule bacteria *(C* and *F)* were allowed to infect bone marrow–derived macrophages for 3 h, and then macrophages were stained for bacteria with anti–*B. anthracis* antibody and were observed by use of a fluorescence *(A–C)* or a phase contrast *(D–F)* microscope. *G,* Mouse bone marrow–derived macrophages incubated for 3 h with wild-type bacteria, *dep* mutant bacteria, cap mutant bacteria, or *dep* mutant bacteria with L-capsule and incubated, fixed, and stained with anti–*B. anthracis* antibody. Infected macrophages were located, and no. of intact bacteria per macrophage was determined. Data are mean ± SD of triplicate samples from 3 identical experiments (total, 9 coverslips) in which 100 infected macrophages were scored per experiment. Bacteria/macrophage, yield of bacteria in an individual macrophage. Percentage of infected macrophages, fraction of 100 infected macrophages that contained the indicated no. of bacteria. Original magnification, ×1000.

ence of 5%–20% CO_2, together with that of the *cap* region [25]. Northern hybridization was performed with probes specific for the 4 genes (figure 3*A*). When RNA was prepared from *B. anthracis* Sm grown in 20% CO_2, all 4 probes hybridized with a transcript of ~6 kb (figure 3*B*). However, no hybridization was observed with RNA from cells grown in a normal atmosphere (figure 3*B*). We concluded that the *cap-dep* region constitutes a single operon whose expression depends on CO_2 concentration, which suggests that these 4 genes might be coexpressed in vivo.

Discussion

After germination, *B. anthracis* endospores change to vegetative forms, which express toxin and capsule genes and eventually, following extracellular growth, cause lethal damage of host cells. Although the germination process and the mode of action of anthrax toxins have been well characterized [26, 27], the mechanisms involved in escaping host defenses during extracellular growth remain undefined. It has been proposed that the capsule of *B. anthracis* protects the bacteria from complement activation and phagocyte-mediated killing, in a manner similar to that seen in other capsulated pathogenic bacteria [25]. In this study, we demonstrated that the L-capsule, which resulted from degradation of the H-capsule by the *dep* gene product and was released from the bacterial cell surface, played an essential role in mediating escape from host defenses, because a *dep* mutant formed normal capsule around its surface but lost pathogenicity for mice (table 1). In fact, when the *dep* mutant was premixed with L-capsule, its virulence for mice was restored. However, although the parent strain was rarely up-

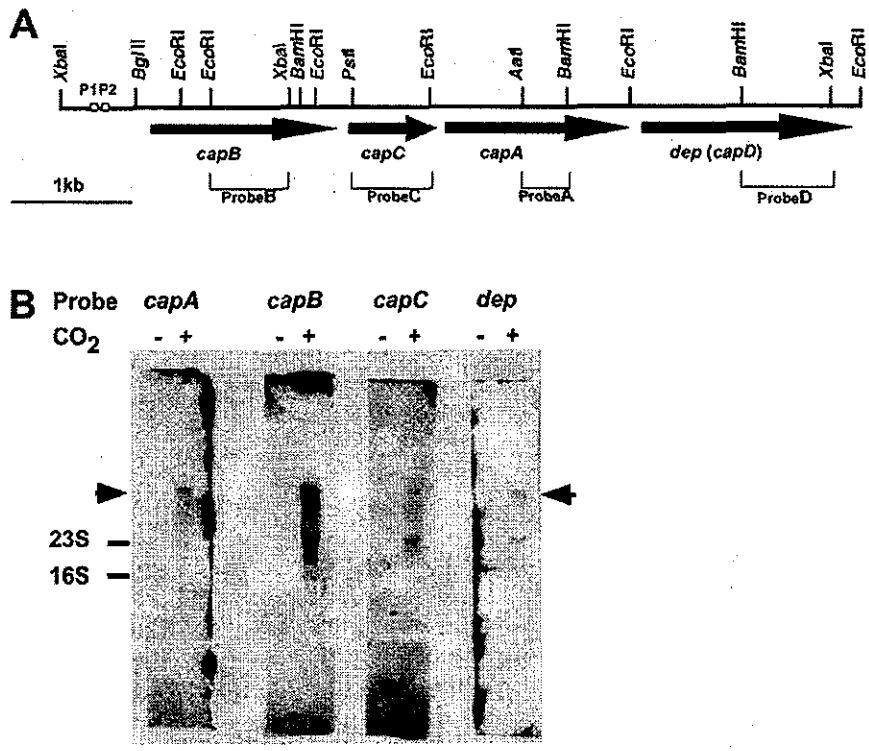

Figure 3. Physical map *(A)* and Northern hybridization analysis *(B)* of *cap-dep* region. Two promoters, P1 and P2, were reported earlier [16]. The 4 DNA probes indicated were constructed with appropriate restriction enzymes *(A)*. The transcript (~6 kb) that hybridized with all 4 probes is indicated *(arrowheads; B)*. RNA samples were isolated from *Bacillus anthracis* Sm broth culture in normal atmosphere (−) or under 20% CO_2 (+), and each 8 μg of the samples was electrophoresed in 1.0% agarose gel. The positions of 23S and 16S rRNA are indicated *(left)*. Although faint bands hybridized with each probe were detected in the lanes at the positions of 23S and 16S rRNA, they were thought to be degraded mRNA of the ~6 kb transcript.

taken by macrophages, the *dep* mutant was efficiently uptaken even if the L-capsule was endogenously mixed in vitro. Therefore, we concluded that the antiphagocytic factor in *B. anthracis* was not the capsule formation but rather was the production of L-capsule in vivo. In addition, the *dep* mutant mixed with L-capsule prereacted with heat-inactivated normal mouse serum regained infectivity for mice, but its infectivity was lost with the capsule prereacted with fresh normal mouse serum (table 1). The capsule of *B. anthracis* thus appears to confer complement resistance during the extracellular growth of vegetative bacilli, and L-capsule released from the cell surface might act as a decoy to protect bacterial cells from complement. This finding, to our knowledge, would be the first report of a novel escape mechanism of bacteria from the host defense system. However, since the loss of the infectivity with normal serum was not complete (table 1), L-capsule might have additional unknown functions against the host defense system.

Five stages of the systemic anthrax infectious cycle have been proposed [8–12, 23, 28]. At the immediate-early stage, bacterial endospores invade the body and undergo rapidly phagocytosis by macrophages, followed by germination and release into the bloodstream. At the middle stage, bacterial cells explosively grow in the bloodstream as extracellular pathogens and actively express virulence factors, followed by stimulation of cytokine production by macrophages and induction of the lethal shock to host cells at the late stage. At the early and middle stages, it is probably too difficult to diagnose anthrax infection. We showed here that *B. anthracis* vegetative forms grow extracellularly and polymerize H-capsule on their surfaces but simultaneously and successively degrade it to L-capsule, which is then released from the cell surface to act as a decoy against the host defense system. Consequently, L-capsule would be essential for the explosive multiplication of *B. anthracis* in vivo. Since no antibiotic therapies would be effective at the late stage of anthrax, the inhibition of the explosive multiplication by removing the L-capsule from the body might be the most effective therapy. Recently, 2 new discoveries lay the groundwork for drugs that could disable the toxin and, along with antibiotics, save lives; the cloning of the human PA receptor, using a genetic complementation approach [29], and the identification of the crystal structure of lethal factor [30]. In addition, the isolation of a synthetic peptide that blocks the action of anthrax toxin in an animal model was reported [31]. In the laboratory, a synthetic version of this receptor or a synthetic peptide might

mop up the poison and protect cells and then might serve as a decoy. When our future trials can incorporate these findings, a useful therapeutic ally against clinical anthrax may be found.

Two promoters, P1 and P2, were identified upstream of *capB* and were activated by high concentrations of CO_2 (figure 3*B*) [17]. We showed here that the *dep* and *cap* genes contained a single transcriptional unit of ~6 kb that was induced by CO_2, similar to that shown for P1 and P2. The *acpA* gene, which is a positive regulator for the *cap* region [20], presumably acts in a similar fashion for the *dep* gene. Indeed, the CO_2-induced expression of *cap* and *dep* may well be a result of the CO_2-induced expression of *acpA* [17, 20]. At the same time, the *atxA* gene product, which is a positive regulator for the toxin genes [18], also positively regulates *cap* gene expression by interaction with a DNA segment 70 bp upstream of the P1 site, as well as the *acpA* gene. Unlike the *acpA* gene, the expression of the *atxA* gene is not controlled by CO_2 [13]. Although it is not known why both *acpA* and *atxA* positively regulate the expression of the *cap* operon, encapsulation seems to protect the bacterial cell from the host defense system via the interaction of various regulatory genes and either CO_2-dependent or -independent expression. *B. anthracis* probably has more regulatory genes. For example, since the expression of the toxin genes was enhanced by CO_2 [14], another CO_2-dependent regulatory gene seems to exist on either the 110 mDa toxin plasmid or the *B. anthracis* chromosome.

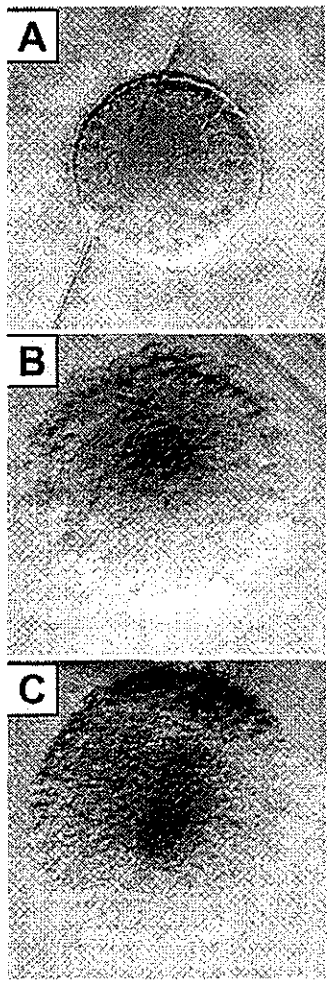

Figure 4. Colonies of *dep*⁻ *Bacillus anthracis*. *B. anthracis* Sm *(A)*, Sm-1 *(B)*, and Sm-3 *(C)* were incubated on NBY agar plates [5] for 24 h at 37°C in an atmosphere containing 5% CO_2, and then colonies were observed by use of a stereoscopic microscope. Original magnification, ×50.

We proposed in this study that, as soon as H-capsule is formed on the bacterial cell surface, it may be simultaneously or sequentially depolymerized to L-capsule. If that was not the case, there would be a time lag between the polymerization and the depolymerization on the bacterial cell surface, and then *B. anthracis* would be easily killed by phagocytosis. Naturally, this speculation is deduced from the results of the present paper, because the *cap* region and the *dep* gene constitute an operon. Moreover, when we observed *B. anthracis* cells grown on the NBY plates by the stereoscopic microscope, the parent strain was smooth, but the *dep* mutant was almost not smooth, although both strains normally formed capsule on the cell surface, and, simultaneously, the shape of the *dep* mutant was different from that of the capsule negative strain (figure 4). Capsular substance appears to accumulate on the cell surface in the *dep* mutant because of the lack of depolymerization. A single-operon structure would be an efficient means of achieving simultaneously the apparently constructing polymerization and depolymerization reactions. The encapsulation process has not yet been defined biochemically, but 3 *cap* genes—*capB, capC,* and *capA,* arranged in that order—are essential for the polymerization, and the *dep* gene is essential for the depolymerization. *B. anthracis* thus seems to have developed an ingenious mechanism to protect itself from host defense mechanisms. Finally, we propose in this paper the new gene designation of *capD,* instead of *dep,* since the gene is a part of the *cap* region, and these genes constitute an operon and perform essential, related biological functions.

Acknowledgment

We are grateful to B. Adler for critical suggestions on the manuscript.

References

1. Beall FA, Taylor MJ, Thorne CB. Rapid lethal effect in rats of a third component found upon fractionating the toxin of *Bacillus anthracis*. J Bacteriol **1962**;83:1274–80.
2. Stanley JL, Sargent K, Smith H. Purification of anthrax toxin factors I and II of the anthrax toxin produced *in vitro*. J Gen Microbiol **1960**;22:206–18.
3. Sterne M. Variation in *Bacillus anthracis*. Onderstepoort J Vet Sci Anim Ind **1937**;8:279–349.
4. Tang G, Leppla SH. Proteasome activity is required for anthrax lethal toxin to kill macrophages. Infect Immun **1999**;67:3055–60.